

266



# Long-Range Forecasting and Climate Research

**Sahel rainfall, Northern Hemisphere  
circulation anomalies and worldwide  
sea temperature changes**

by

**C.K. Folland, D.E. Parker, M.N. Ward  
and A.W. Colman**

7A

L 507A (Amended July 1987)

**September 1986**

Meteorological Office (Met. O. 13)  
London Road  
Bracknell  
Berkshire RG12 2SZ

ORGS UKMO L

**National Meteorological Library**  
FitzRoy Road, Exeter, Devon. EX1 3PB

METEOROLOGICAL OFFICE  
152395  
17 JUN 1988  
LIBRARY

LONG RANGE FORECASTING AND CLIMATE  
RESEARCH MEMORANDUM NO 7A

SAHEL RAINFALL, NORTHERN HEMISPHERE CIRCULATION ANOMALIES  
AND WORLDWIDE SEA TEMPERATURE CHANGES

by

C K FOLLAND, D E PARKER, M N WARD AND A W COLMAN

MET O 13 (SYNOPTIC CLIMATOLOGY BRANCH)  
METEOROLOGICAL OFFICE  
LONDON ROAD  
BRACKNELL  
BERKSHIRE RG12 2SZ

SEPTEMBER 1986  
AMENDED JULY 1987

NOTE. This paper has not been published. Permission to quote from it should be obtained from the Assistant Director (Synoptic Climatology), Meteorological Office.

STUDY WEEK ON PERSISTENT METEO-OCEANOGRAPHIC ANOMALIES  
AND TELECONNECTIONS, PONTIFICAL ACADEMY, VATICAN, 23-27 SEPT 1986.  
SAHEL RAINFALL, N. HEMISPHERE CIRCULATION ANOMALIES AND WORLDWIDE SEA  
TEMPERATURE CHANGES

by C K Folland, D E Parker, N Ward and A Colman  
Meteorological Office, Bracknell, UK

ABSTRACT

We present observational evidence of decadal time scale fluctuations of world-wide SST anomalies in all seasons of the year during this century. The most prominent fluctuation on this time scale since 1950 has included a relative fluctuation of SST between the oceanic hemispheres. This fluctuation has been accompanied by significantly changed circulation patterns over most of the N. Hemisphere in most months of the year; the details of these changes vary only slowly with season. Northwestern Europe, for example, has been quite strongly affected, especially in summer. An even more compelling association is that with Sahel rainfall. Model experiments confirm that summer Sahel rainfall is almost certainly affected by large scale SST patterns. The model results are presented in detail in a companion paper by Palmer (1986b); only the most salient results are reproduced here.

Interannual as well as interdecadal variations of large scale SST are used to design two statistical forecasting models that attempt to predict summer Sahel rainfall from SST anomaly patterns (referred to as SSTA below) observed in previous months. The likely longer-term skill of the forecasting models is discussed. In June 1986, the first experimental rainfall forecast for the Sahel was issued to African countries (WMO Region I) by the UK Meteorological Office for the summer 1986 season; the performance of this forecast is briefly reviewed to date.

Finally, we summarise ongoing observational and modelling studies in the Meteorological Office which are designed to explore the consequences of observed large scale SST changes for Sahel rainfall and other climate fluctuations in more detail.

## 1. Introduction

The Meteorological Office possesses one of the best quality-controlled sea surface temperature (SST) data sets at present available (Minhinick and Folland (1984); Parker et al (1987)). The SST data set, formerly known as MOHSST (Meteorological Office Historical Sea Surface temperature data set) is now a component of MOST (Meteorological Office Ocean Surface Temperature Data sets) which includes several marine air temperature sets; MOST is continuously updated in near real time (Parker et al (1987)). The data sets form a central component of a wide-ranging research program into the physical basis of low-frequency weather and climate variation and into practical monthly and seasonal forecasting using general circulation models and globally distributed observations. The instrumental corrections used in this paper for SST prior to 1942 are those published in Folland, Parker and Kates (1984).

Anomalies of atmospheric circulation, especially in the N. Atlantic sector, are known to have been large at certain seasons over epochs as long as decades and to have been accompanied by large scale SST variations. Examples include changes of atmospheric circulation over the N. Atlantic in winter, especially between early twentieth century decades and recent decades (Lamb 1972, Makrogiannis et al (1982), Folland, Parker and Newman (FPN) (1985)); changes in Central England temperature in October (warmer) and April (colder) in recent decades (Gilchrist (1982), FPN (1985)); and a tendency for reduced rainfall over UK in July and August since about 1965. Fig 1 shows graphs of Central England Temperature (Manley (1974)) for April and October plotted in the form of a 20 year running average (the series has been updated by Storey, Folland and Parker (1985)).

The interannual variability of atmospheric circulation patterns is certainly accompanied by interannual SST changes (although the extent of a direct influence is uncertain). Best known are the interactive effects of El Nino and the atmosphere (eg Palmer and Mansfield (1986), Gill and Rasmusson (1983). These interactions, (most prominent in the Pacific), are likely to have a near global scale component if only because the SST changes sometimes develop on this scale (Hsiung and Newell (1983), Pan and Oort (1983), FPN (1985)). On the regional scale fluctuations in the interface between the Gulf Stream and the Labrador Current have been onvincingly shown to influence circulation in winter over the N Atlantic and Europe via a positive ocean-atmosphere feedback (Palmer and Sun (1985), Ratcliffe and Murray (1970)).

We can gain a "feel" for the worldwide effects of SST anomalies on the atmosphere using the simple physical arguments of Sawyer (1965) about the likely magnitude of the effects of SST anomalies on the atmosphere. For example imagine a truly worldwide pattern of SST changes to be suddenly "switched on" whose regional scales of anomalies having a similar sign are approximately those of the largest scale features of the atmosphere. Let the mean modulus of the anomalies be  $0.3^{\circ}\text{C}$ . Assuming that the atmosphere is initially in its "climatological mean state", this pattern of SSTA would provide anomalous heating of these atmospheric scales with a mean modulus of about  $10 \text{ Wm}^{-2}$  over the 70% of the globe that is ocean. The local magnitude of the heating change would vary from zero to substantially larger values.

No change in average heating is necessarily implied here, only a change in its spatial distribution.  $10 \text{ Wm}^{-2}$  is about 10% of the change in the large scale heating of the atmosphere by the oceans during the seasonal cycle; [we can imagine changes in ice cover are included]. So world wide changes of SST of this magnitude, which may not involve a globally averaged SST change, or regional changes of considerably larger magnitude (such as those

associated with El Nino), can be seen as potentially large enough to effect the global atmospheric circulation.

Using MOST data, Fig 2 shows a time-series of the areal-mean modulus of the changes between successive years of July and August combined SST anomaly between 1951 and 1980 on the 20 x 20 degree (approximately  $3 \times 10^6 \text{ km}^2$ ) space scale over about 70% of the world ocean (there are few data south of  $45^\circ \text{S}$ ). The two month time scale is of special interest because models run in a perpetual single-season mode indicate that the atmosphere tends to come into a near equilibrium with large scale SST changes, certainly in the tropics, in about two months (example in Folland et al (1987)). The downwards trends in Fig 2 may be the result of gradually improving data. An interannual change with a mean magnitude of  $0.48^\circ \text{C}$  is large enough to affect the atmosphere, and therefore the SSTA changes may be large enough to affect regional scale climate on the interannual time scale in most years. This value may be compared with the value of  $0.46^\circ \text{C}$  that corresponds to the SST difference field for July to September on a 5 x 5 degree space scale (Fig 3) used in the Sahel modelling experiments of Folland, Palmer and Parker (1986) (FPP).

Table 1 shows the values of two decadal averaged indices (a) the anomalies in global mean SST (July to Sept) (b) those of the Southern Hemisphere with the Northern Indian Ocean SST (SHNI) minus remainder of the N Hemisphere SST (RHN) (July to Sept). These "slow" global scale SST changes (note their differing relative importance in different epochs) are thus about as important as the interannual two-month time scale changes on a twenty year time scale. Both appear to be of sufficient magnitude to affect the atmosphere. Therefore we suggest that the effects of observed interannual and interdecadal SST variations on regional atmospheric circulation may have been of comparable importance over the last century or so. Because the atmospheric mean flow is different in different seasons (and often in different calendar months) then it might be expected that the atmosphere would respond to these boundary value variations in a manner that varies with season. In transition seasons the atmospheric response may change appreciably from one calendar month to another. Changes in the mean circulation may be easy to discover but accompanying changes in the probability of regional circulation and surface weather extremes are more likely to be of practical importance. Section 5 describes forecasts of summer Sahel rainfall and an attempt is made to predict the probabilities of possible rainfall outcomes.

## 2. Worldwide patterns of SST change since 1901

Figs 4a, 5a, 6a show the first three covariance eigenvectors of seasonal mean worldwide SST anomalies (from a 1951-80 average) calculated over all available 10 x 10 degree areas for 1901-80, and Figs 4b, 5b, 6b (dotted lines) show time series of the eigenvector coefficients from 1901-1986. The EOF's were constructed using data for all seasons together. Season 1 is December-February, season 2 March to May etc. Missing data have been "filled in" using Chebychev polynomials to interpolate in time. A 10 x 10 degree anomaly in a given season is regarded as being present if at least one constituent 5 x 5 degree anomaly is available. A full description of the technique will appear in a later paper. To show that these EOF's represent real physical properties, Figs 4b, 5b and 6b also show time series (1901-85) of (4b) global mean in all seasons, (5b) mean SST for tropical E. Pacific (SST is plotted one season prior to that of EOF2), and (6b) Sahel rainfall (Nicholson (1985)) plotted against the values of EOF3 in June to August. The correlations of the EOF series with the series chosen for comparison are highly significant (significance values shown on diagrams are

highly significant assuming 40 degrees of freedom). In fact EOF1 is an excellent representation of the relative importance of worldwide SST changes since 1901, EOF2 is a good representation of the worldwide effects of El Nino (FPN(1985)) and EOF3 "represents" the interhemispheric SST anomalies simultaneously associated with those of Sahel rainfall on the interannual (to some extent) as well as interdecadal time scales (FPP 1986). EOF3 is fairly similar to the SST difference field (Fig 3) used by FPP in their modelling experiments (described in more detail in the companion paper by Palmer (1986b)) which show a prima facie case for the physical reality of a connection between Sahel rainfall and worldwide SST. So we may regard EOF3 as one of the principal patterns of SSTA that influences Sahel rainfall. We now discuss the problem of Sahel rainfall from an observational viewpoint in more detail.

### 3. Sahel rainfall and Worldwide SST variations

Rainfall records for sub-Saharan North Africa have been collated and normalized by many authors. We have used an updated version of Nicholson's (1980, 1985) annual Sahel series for 1901-84 (Fig 7a) supplemented by CLIMAT reports for 1985. Fig 7b gives a map of the area, which stretches from Senegal to Sudan at approximately 14-18 N. Nicholson tried to homogenize her rainfall data to allow for the use of widely differing numbers of stations through time; the least reliable estimates are likely to be before 1919 and very recent ones.

Most rain falls in June or July to September or October and is associated with the seasonal movement of the Intertropical Convergence Zone (ITCZ). FPP and Palmer (1986a) suggest that the worldwide pattern of SST anomalies represented by Fig 6a (EOF3) modulates the intensity of the moisture flux convergence into the Intertropical Convergence Zone and to a limited extent modulates the latitude of the convectively active region of that zone. It is probable that the surprising sensitivity of the Sahel rainfall climate to SST is the result of a strong local positive feedback from soil moisture during the wet season (Walker and Rowntree (1977) (high moisture flux convergence - wetter soil - more evaporation - more local precipitation etc) and even from seasonal variations in albedo (wetter soil gives darker soil and/or greener vegetation etc), though there is no direct proof of the latter effect. An important question is: could summer Sahel rainfall be predicted in advance from SSTA observed in the previous months?

FPP indicated that the spatial scale of SSTA that simultaneously affect the Sahel is considerably larger than that of the tropical N and S Atlantic anomalies as originally discussed by Hastenrath (1984) Lamb (1978) and Lough (1981). This is well illustrated by Table 2. Although large scale SSTA cannot be the only controlling factor, the type of SSTA pattern represented by EOF3 has probably had (see Fig 6b) quite a strong influence on Sahel rainfall throughout the period 1901-85. The suggestions by Lough (1981, 1986) that different factors influenced Sahel rainfall (and areas further south) prior to 1940 compared with the post war period may be correct but Lough's arguments only referred to the influence of the tropical Atlantic. However it is unlikely that the SSTA pattern of Fig 6a (EOF3) is the only large scale SSTA pattern that influences Sahel rainfall.

In the current state of knowledge early progress in predicting Sahel rainfall may depend on the extent to which the many degrees of freedom in worldwide SSTA can be represented by a few important worldwide SST patterns which can occur prior to the Sahel wet season and modulate Sahel rainfall.

This possibility is suggested by a statistically significant correlation ( $r = 0.58$ , significant at 99.9% level assuming 40 degrees of freedom), between the coefficients of EOF3 measured in March-May and the subsequent "summer" rainfall in the Sahel measured over the period 1901-85. Fig 8 shows Nicholson's Sahel series plotted against the March-May coefficients of EOF3 for the period 1901-85. The good correlation may be a result of the persistence of this and perhaps other worldwide SSTA patterns between seasons (though exact persistence is not required, only that a characteristic SSTA pattern in, say, March-May precedes a given, perhaps different, SSTA pattern in July-September).

#### 4. Changes of N. Hemispheric Atmospheric circulation since 1950

Inspection of Fig 7a shows that, in the last few decades, interdecadal fluctuations in Sahel rainfall have been especially large. We now believe that an important reason for the clear increase in the interdecadal component of Sahel rainfall fluctuations is a pattern of relative changes in SST between the hemispheres which commenced about 1955 and appears in all seasons. This is illustrated by Figs 9a-9d which show the SST changes (1968-84) minus (1950-59) for (i) January (ii) April (iii) July and (iv) October. It is extremely difficult to estimate the statistical significance of the changes but an attempt has been made using the conservative Fisher Behrens "t" test. The "significant" areas (at the 5% level) are indicated by boxing. These cover 11-19% of the area (Table 3). The mean modulus of the difference in SST between these two periods (20 x 20 degree areas) in July is  $0.31^{\circ}\text{C}$ . Following the arguments of Section 1, this is likely to correspond (approximately) to a change of the pattern of atmospheric heating in July of mean modulus  $10 \text{ Wm}^{-2}$  in 1968-84 when applied to an atmosphere in "equilibrium" with the 1950-59 SST field. This is about 10% of that due to the annual cycle of worldwide SST between February and August. Other months show broadly similar results.

Fig 10a-f show, not unexpectedly, that this change may have been sufficient to affect much of the extratropical N. Hemisphere atmospheric circulation. Here the difference in pressure at mean sea level (PMSL) between 1968-84 and 1950-59 is drawn for March, April, May, July, August and October. Strongly significant changes are also shown in 500 mb height.

Table 3 indicates the spatial extent of statistically significant areas on the PMSL and 500 mb difference maps. Lack of homogeneity of the PMSL data may have influenced the results, especially over the Southern Rocky Mountains and over Tibet (Williams and van Loon (1976)\*). Nevertheless a fairly coherent picture emerges of changes from month to month in the PMSL patterns which tend to be largest and often significant in the best observed region - the mid latitude N. Atlantic/European sector. The SST changes are clearly even more coherent (Fig 9). Fig 11 shows the mean PMSL changes for the winter (December-March), and for the remainder of the year; these monthly variations have had very evident effects on UK weather, especially in April, May, July, August, October and November.

Fig 12 shows a time-series of rainfall (based on about 200 stations) for England and Wales in July and August; the series was homogenised by Wigley et al (1984) and updated in the Synoptic Climatology Branch of the Meteorological Office. The pattern of SST changes was sufficiently regular

\* Our recent investigations of the PMSL data suggest that they are likely to be unreliable in surrounding regions also. See footnotes in Figures 10 and 11.

that the difference in rainfall over England and Wales between the consecutive periods 1950-67 and 1968-85 was exactly 1 standard deviation (as calculated over the period 1901-80) and significant at at least the 99% level (assuming 10 degrees of freedom in a standard pair "t" test). Fig 13 shows a time-series of mean July and August PMSL at 55 N 10 W plotted against the SST index SHNI minus RNH (July-Sept) (see Table 1 for definition) and also against Sahel rainfall for 1901-85. The correlation of these series is shown on Fig 13; all correlations (assuming 40 degrees of freedom) are highly significant. A cross spectral analysis (not shown) indicates that PMSL at 55 N 10 W (corresponding to the high pressure anomaly in Figs 10d and 10e) is strongly positively correlated with the other time series in Fig 13 on the interdecadal time scale but rather more weakly on interannual time scales. This is to be expected given the large internal variability of the mid-latitude atmosphere. Further details can be found in Folland, Parker and Palmer (1985).

#### 5. Forecasting Sahel rainfall from Worldwide SST anomalies by empirical models

In June 1986, the Meteorological Office issued an experimental long-range forecast of rainfall over the Sahel for the summer of 1986. This very cautiously worded forecast arose from the research on the relationships between Sahel rainfall and worldwide SST discussed above and the supporting general circulation model results in FPP and in Palmer (1986a). Two techniques of forecasting have been devised and tested on independent data:

- (a) A regression technique which relates worldwide SST anomalies in the N. Hemisphere spring to Sahel rainfall in the following summer. The technique provides a "deterministic" forecast whose uncertainty can be fairly readily quantified.
- (b) A technique based on the use of linear discriminant prediction. This provides a forecast of the probability of each of five categories of Sahel rainfall using up to eight predictors. These predictors are (currently) coefficients of covariance eigenvectors of worldwide SSTA of the type described in Section 2: 2 sets of eigenvectors were calculated, using the periods 1901-80 and 1951-80 respectively. A coefficient time series for each eigenvector was calculated over the period 1901-86.

##### Method (a)

We first calculate the linear regression between Sahel rainfall and locally observed values of SSTA covering much of the globe over some fixed period prior to the Sahel rainfall season. The local SSTA are measured over 5 x 5 degree or 10 x 10 degree areas; the regression relationships are calculated from data measured within the period 1901-84. Fig 14a shows an example of a regression map for 1946-84 that relates March-May SSTA to the following summer's Sahel rainfall; here we show the values of slopes of the regression coefficients that relate Sahel rainfall to the local values of SSTA.

The next stage is to calculate for each year the covariance of the worldwide SSTA field with the regression-slope field for the same calendar period for a set number of years selected as the model's "training period". This provides a measure of the similarity of the SSTA pattern in a given year to the pattern of the regression-slope field. Finally we calculate a new regression equation that relates the values of this covariance factor to

Sahel rainfall in the following summer over the training period. This equation can then be used in years subsequent to the training period to forecast the summer Sahel rainfall by measuring the covariance between the observed SSTA field and the fixed regression-slope field in for example the spring of the year for which a forecast is required. Fig 14b shows predictions for 1981 to 1986 made using two versions of this model. A more extensive discussion of the technique, with statistical simulations on independent data, is given in Parker et al (1986).

#### Method (b)

The linear discriminant prediction technique (see Afifi and Azen (1979) for a fundamental description of discriminant analysis) also requires that a training period be specified. Sahel summer (July-September) rainfall amounts within the training period are divided (in current models) into equiprobable ranges ("Quints"); their boundaries (quintiles) are derived from the training period. This is necessary as the linear discriminant prediction equations are more stable if equal numbers of observations of the values of each predictor are available in each of the predefined ranges.

Five linear discriminant equations are calculated using a stepwise technique. The equations relate the observed occurrence of each quint in the training period to the values of the coefficients of a set of worldwide SST eigenvectors which are measured over a fixed period in the Spring prior to each Sahel rainfall season. The 5 equations forecast the probability of each quint respectively in the coming season using normal distribution theory and Bayes' theorem. This technique is formally similar to but less complex than the multivariate forecasting technique used in monthly long-range forecasting for the UK (Folland and Colman (FC) (1986), Folland and Woodcock (1986)). The "best" a priori model is chosen using a "jackknife test" (see FC (1986)). Quite high jackknife "hit rates" have been found in some of these models (a "hit" is said to occur when the observed quint category is the same as the quint forecast to have highest probability). One set of models has been based on a 1901-85 training period using eigenvectors based on the period 1951-80. This model gave a hit rate of 40% and an "F" value of 15 for the significance of the 1951-80 EOF2 (quite like the 1901-80 EOF3, Fig 6a) as a discriminant predictor. Table 4a shows the result of an attempt by a model using the same data as the model described above but with a 1901-67 training period and 1901-80 eigenvectors to "predict" the Sahel drought years from 1968-85. The results are encouraging though "quint 1" based on 1901-67 is not very dry (-0.3 based on Nicholson's measure of Sahel rainfall, Fig 7a).

Tables 4b and 4c show some predictions for 1981-6 based on shorter training periods but using quint rainfall categories better matched to the present drier Sahel rainfall climate. The predictions are encouragingly successful with most years (1981-85) well predicted. Tables 4a and 4b show occasional gross failures of the models. Indeed these failures underline the need to look more deeply into the statistics of "Sahel rainfall" (rainfall anomalies over the Sahel are not always homogeneous as shown by Nicholson (1980)) as well as other physical processes that affect Sahel rainfall. Nevertheless it is clear that large scale SST fluctuations have an important controlling influence over rainfall in sub-Saharan Africa. The special importance of regional SST anomalies also requires urgent investigation.

## 6. Conclusion and Projected Work

We believe we have provided a strong case that coherent large scale SST changes occur, that they modulate Sahel rainfall and N. Hemisphere atmospheric circulation, and that they have potential for use as predictors in forecasting Sahel rainfall. In addition, worldwide SSTA (measured in limited but widely spread regions) are found to be useful as predictors for the extratropics (for monthly PMSL pattern forecasts in the region of the UK).

We see that the next step is to include a more realistic set of general circulation model experiments which should be designed to study in better detail physical processes which affect Sahel rainfall and involve contrasting worldwide SST anomalies. We have started some "partial annual cycle" experiments running from modelled "Aprils" to "Octobers" using globally complete sequences of observed monthly SST anomalies in those months in selected years. The years will include 1950 and 1984 and are being chosen for their extremes (wet or dry) of Sahel rainfall and for contrasting worldwide SST patterns (Fig 15). Fig 16 shows initial results from model experiments representative of 1950, a very wet year in the Sahel. The changes in rainfall, when compared with the model's climatology, are in good qualitative agreement in each month from June to September with observations for these months published by Dennett et al (1985). The model was initialised using atmospheric data for the end of March 1984 and the first two months of the integration have been discarded because at least a month is required for the model to resolve the initial disequilibrium imposed by the SST forcing.

The historical SST data are also being improved. The most immediate activity is the estimation of seasonally and geographically varying corrections for the biases of uninsulated sea temperature buckets using a developed form of the scheme suggested in Folland and Hsiung (1986). An initial picture of the proposed corrections for August is shown in Fig. 17; the average global correction is slightly less than in FPK but what is much more important is a range in the regional values of the corrections of about  $0.5^{\circ}\text{C}$ . Their pattern seems likely to influence the amplitude of EOF3 before 1942 (when the corrections were applied).

We are also carrying out a more detailed study of the atmospheric circulation variations over the extratropical N. Hemisphere (PMSL, 500 mb height and 500 mb - 1000 mb thickness). Daily data (1946-1986) are being filtered on several time scales from less than six days to 25-80 days. A rotated eigenvector analysis of some of these data is also planned because Barnston and Livezey (1985) have indicated that this may be a useful way of identifying some of the characteristic patterns associated with low frequency atmospheric variability described by many authors (eg Blackmon and Wallace (1983)).

Finally the interhemispheric SST variations discussed in the paper may be the result of cooperative ocean atmosphere interactions on time scales of up to several decades. Initial work on the formulation of hypotheses to explain these changes will be discussed in Folland et al (1987).

- Afifi, A A and Azen, S P 1979 Statistical analysis - a computer - orientated approach. Second Ed., Academic Press.
- Barnston A G and Livesey H E 1985 High resolution rotated empirical orthogonal function analysis of northern hemisphere 700 mb heights for predictive purposes. 9th Conf. Prob. Stat. Atmos. Sci., Boston, Mass, 290-297
- Blackmon, M L and Wallace, J M 1983 On the structure and time evolution of low frequency atmospheric fluctuations Proc. 7th Ann. Clim. Diagn. Workshop 311-318
- Bottomley, M., Folland, C K, Hsiung, J. Newell, R E and Parker, D E 1987 Global Ocean Surface Temperature Atlas (GOSTA). HMSO/MIT. In preparation.
- Dennett, M D, Elston, J and Rodgers, J A 1985 A reappraisal of rainfall trends in the Sahel. J. Clim., 5, 353-361
- Folland, C K and Colman, A 1986 A multivariate technique for use in long-range forecasting. WMO Long-Range Forecast Res. Rep. Ser. No. 6.Vol II, 627-636
- Folland, C K and Hsiung, J 1986 Corrections of seasonally-varying biases in uninsulated bucket sea surface temperature data using a physical model. Met O 13 Branch Memorandum No 154, Meteorological Office, Bracknell, England
- Folland, C K, Palmer, T N and Parker, D E 1986 Sahel rainfall and worldwide sea temperatures, 1901-1985. Nature, 320, 602-607
- Folland, C K, Parker, D E and Kates, F E 1984 Worldwide marine temperature fluctuations 1856-1981. Nature, 310, 670-673
- Folland, C K, Parker, D E and Newman, M R 1985 Worldwide marine temperature fluctuations on the season to century time scale. Proc. 9th Climate Diagnostics Conference, Corvallis, Oregon, 22-26 Oct' 1984, 70-85
- Folland, C K, Parker, D E and Palmer, T N 1985 Sahel drought and worldwide sea surface temperature. MRSCP/12 Meteorological Office Bracknell England
- Folland, C K, Parker, D E Wigley, T M L, Jones, P D and Palmer, T N 1987 Warming of the southern hemisphere in recent decades. For Proc. WCRP conf. on Mech. of interannual and longer-term climate variation. Melbourne, 8-12 Dec 86
- Folland, C K and Woodcock, A 1986 Experimental monthly long-range forecasts for the United Kingdom, Met Mag., 115, 301-318.
- Gilchrist, A 1982 Long Range forecasting in the Meteorological Office, Part I, II, ECMWF Semin. Probl. Prospect. Long Med. Range Weather Forecast, 1981, 21-54
- Gill, A E and Rasmusson, E M 1983 The 1982-82 climate anomaly in the equatorial Pacific. Nature, 306, 229-234

- Hastenrath, S 1984 Interannual variability and annual cycle: mechanisms of circulation and climate in the Tropical Atlantic sector. Mon. Weath. Rev., 112, 1097-1107
- Hsiung, J and Newell, R E 1983 The principal non-seasonal modes of variations of global sea surface temperatures. J. Phys. Ocean., 13, 1957-1967
- Lamb, H H 1972 Climate: Present, Past and Future. Vol. I. Methuen
- Lamb, P J 1978 Large scale tropical Atlantic surface circulation patterns associated with sub-saharan weather anomalies. Tellus, 30, 240-251
- Lough, J M 1981 Atlantic sea surface temperatures and weather in Africa. PhD thesis, Univ East Anglia
- Lough, J M 1986 Tropical Atlantic sea surface temperatures and rainfall variations in Sub-saharan Africa. Mon. Weath. Rev., 114, 561-570
- Makrogiannis, T J, Bloutsos, A A and Giles, B D 1982 Zonal index and circulation change in the North Atlantic area, 1873-1972. J. Clim, 2, 159-169
- Manley, G 1974 Central England temperatures: monthly means 1659 to 1973. Q. J. R. Met. Soc., 100, 389-405
- Minhinick, J M and Folland, C K 1984 The Meteorological Office historical sea surface temperature data set. Met O 13 Branch Memorandum No 137, Meteorological Office, Bracknell, England
- Nicholson, S E 1980 The nature of rainfall fluctuations in subtropical West Africa. Mon. Weath. Rev., 108, 473-487
- Nicholson, S E 1981 Rainfall and atmospheric circulation during drought periods and wetter years in West Africa. Mon. Weath. Rev., 109, 2191-2208
- Nicholson, S E 1985 Sub-saharan rainfall 1981-84. J. Clim. App. Met., 24, 1388-1391
- Palmer, T N 1986a Influence of the Atlantic, Pacific and Indian Oceans on Sahel rainfall. Nature 322, 251-253

- Palmer, T N 1986b Drought, sea surface temperatures and atmospheric teleconnections. Proc. Study Week on persistent meteo-oceanographic anom. and telecon. 23-27 Sept 1986, Vatican city.
- Palmer, T N and Mansfield D A 1986 A study of winter time circulation anomalies during past El Nino events using a high resolution general circulation model. II: Variability of seasonal mean response. Q. J. R. Met. Soc., 112, 613-638
- Palmer, T N and Sun, Z 1985 A modelling and observational study of the relationship between sea surface temperature in the north-west Atlantic and the atmosphere general circulation, Q. J. R. Met. Soc., 111, 947-975
- Pan, Y H and Cort, A H 1983 Global climate variations connected with sea surface temperature anomalies in the eastern equatorial Pacific Ocean for the 1958-73 period. Mon. Weath Rev., 111, 1244-1258
- Parker, D E, Greenslade, R and Folland, C K 1986 The stability of statistical relationships between sub-saharan rainfall and worldwide sea surface temperature. Met O 13 Branch Memorandum No 166, Meteorological Office, Bracknell, England
- Ratcliffe, R A S and Murray, R 1970 New lag associations between North Atlantic sea temperature and European pressure applied to long-range weather forecasting. Quart. J R Met Soc, 96, 226-246
- Sawyer J S 1965 Notes on the possible physical causes of long-term weather anomalies. WMO No. 162 T P 79, Tech. Note No 66, 227-248
- Storey, A, Folland, C K and Parker, D E 1985 A homogeneous archive of daily central England temperature 1772 to 1985 and new monthly average values 1974 to 1985. Met O 13 Branch Memorandum No 107, Meteorological Office, Bracknell, England
- Walker, J and Rowntree, P R 1977 The effect of soil moisture on circulation and rainfall in a tropical model Q J R Met Soc., 103, 29-46

Wigley, T M L, Lough, J M and Jones, P D 1984 Spatial patterns of precipitation in England and Wales and a revised, homogeneous England and Wales precipitation series J Clim, 4, 1-25

William, J and Van Loon, H 1976 An examination of the Northern Hemisphere sea-level pressure data set. Mon. Weath. Rev., 104, 1354-1361

## List of Figures

- Figure 1 Long-term changes in central England Temperature in April and October.
- Figure 2 Mean modulus of interannual changes in combined July and August SST anomaly. (Calculated on a  $20^{\circ} \times 20^{\circ}$  spatial scale).
- Figure 3 Difference in July to September SST between five driest and five wettest Sahel wet seasons (1950-1984).
- Figure 4a First eigenvector of worldwide SST anomaly variation, 1901-1980
- Figure 4b Coefficient of the first eigenvector of worldwide SST anomaly variation in Figure 4a (dashed line), and global average SST anomaly (solid line). Values are for successive seasons (Dec-Feb etc). Correlation between the two series: 0.91 (t-value, 13.8: significance  $\ll 10^{-8}\%$ ).
- Figure 5a Second eigenvector of worldwide SST anomaly variation, 1901-1980.
- Figure 5b Coefficient of the second eigenvector of worldwide SST anomaly variation in Figure 5a (dashed line), and average SST anomaly in the E Tropical Pacific ( $20^{\circ}\text{N}$ - $20^{\circ}\text{S}$ ), east of  $170^{\circ}\text{W}$  (solid line). Values are for successive seasons (Dec-Feb etc). Correlation between the two series: 0.65 (t-value, 5.4: significance  $2 \times 10^{-4}\%$ ). (EOF leads by one season)
- Figure 6a Third eigenvector of worldwide SST anomaly variation 1901-1980.
- Figure 6b Coefficient in June to August of the third eigenvector of worldwide SST anomaly variation in Figure 6a (dashed line), and Sahel rainfall (which falls mainly in July to September) (solid line). Correlation between the two series: 0.60 (t-value, 4.75: significance,  $2 \times 10^{-3}\%$ ).
- Figure 7a Standardized annual rainfall anomalies for the Sahel, 1901-1985 (upper panel). Values to 1984 are after Nicholson (1985): 1985 values are from CLIMAT reports. The lower panel gives the number of stations used.
- Figure 7b Sahel rainfall stations used by Nicholson.
- Figure 8 Coefficient in March to May of the third eigenvector of worldwide SST anomaly variation in Figure 6a (dashed line), and Sahel rainfall (solid line). Correlation between the two series: 0.58 (t-value, 4.50: significance,  $3 \times 10^{-3}\%$ ).
- Figure 9a Sea surface temperature, 1968-84 minus 1950-59, January
- Figure 9b Sea surface temperature, 1968-84 minus 1950-59, April
- Figure 9c Sea surface temperature, 1968-84 minus 1950-59, July
- Figure 9d Sea surface temperature, 1968-84 minus 1950-59 October
- Figure 10a MSL Pressure, extratropical N Hemisphere, 1968-84 minus 1950-59 March.

- Figure 10b MSL Pressure, extratropical N Hemisphere, 1968-84 minus 1950-59 April.
- Figure 10c MSL Pressure, extratropical N Hemisphere, 1968-84 minus 1950-59, May.
- Figure 10d MSL Pressure, extratropical N Hemisphere, 1968-84 minus 1950-59, July.
- Figure 10e MSL Pressure, extratropical N Hemisphere, 1968-84 minus 1950-59, August.
- Figure 10f MSL Pressure, extratropical N Hemisphere, 1968-84 minus 1950-59, October.
- Figure 11a MSL Pressure, extratropical N Hemisphere, 1968-84 minus 1950-59, December to March.
- Figure 11b MSL Pressure, extratropical N Hemisphere, 1968-84 minus 1950-59, April to November.
- Figure 12 Standardised England and Wales July and August rainfall, 1901-85.
- Figure 13.1 Mean MSL pressure at  $55^{\circ}\text{N}$   $10^{\circ}\text{W}$  in July and August (——).
- ii Annual Sahel rainfall (-----).
- iii July to September SST, S Hemisphere with N Indian Ocean minus rest of N Hemisphere (——).
- Correlations between series:    1.    vs ii)    :    +0.29  
     1.    vs iii) :    -0.53  
     ii.   vs iii) :    -0.63
- Figure 14a Regression slope of march to May SST on Sahel rainfall, 1945-84. Values are in 10ths  $^{\circ}\text{C}$  per standard deviation of Sahel rainfall.
- Figure 14b Observed Sahel rainfall, 1965-85: and predicted values, 1981-6, using regression technique. The bars on the predictions give the 95% confidence limits.
- Figure 15 SST anomalies, August 1950. Values are in 10ths  $^{\circ}\text{C}$ .
- Figure 16 Monthly deviations of rainfall (mm) from climatology of numerical general circulation model forced by SST anomalies for 1950.
- Figure 17 Corrections to August SST deduced from model of thermodynamics of an uninsulated bucket. Values are in 100ths  $^{\circ}\text{C}$  and have been smoothed 1:2:1 east-west then north-south.

	Globe	SHNI-RNH
1901-10	- 0.37	+ 0.03
1911-20	- 0.33	+ 0.17
1921-30	- 0.24	- 0.08
1931-40	- 0.11	- 0.09
1941-50	- 0.03	- 0.07
1951-60	+ 0.04	- 0.14
1961-70	- 0.02	- 0.08
1971-80	- 0.01	+ 0.20

Table 1 Decadal mean July to September SST anomalies (wrt 1951-80) for the globe and for Southern Hemisphere with N. Indian Ocean, minus the rest of the N. Hemisphere.

Table 2 Correlation of July to September SST time series and Sahel rainfall, 1901-84

No.	Ocean SST series	<i>r</i>	<i>S</i>	$\sigma_0$ (°C)	<i>c</i>	<i>m</i>
1	Southern minus Northern hemisphere	-0.56	**	0.18	-0.15	-1.69
2	SHNI-RNH	-0.62	***	0.19	-0.15	-1.78
3	South-North Atlantic (0-30° S, 0-30° N)	-0.36		0.32	-0.19	-0.60
4	South-North Atlantic	-0.44	*	0.32	-0.24	-0.75
5	As 4 but with division at 5° N	-0.46	*	0.32	-0.25	-0.77
6	South Atlantic+S. Indian+N. Indian+East Tropical Pacific-N. Atlantic-N. Pacific-Mediterranean	-0.67	***	0.96	-0.23	-0.38
7	As 6 but ocean areas weighted according to size	-0.62	***	0.26	-0.09	-1.26
8	As 6 but with Atlantic split at 5° N	-0.69	***	0.96	-0.23	-0.39

*r*, Correlation coefficient; *S*, significance of *r* (assuming only 32 degrees of freedom because of lag-autocorrelation). \*, = 95%; \*\*, = 99%; \*\*\*, = 99.9%;  $\sigma_0$ , Standard deviation of SST series (°C); *c*, regression constant (units are standardized Sahel rainfall); *m*, regression slope.

MONTH	PERCENTAGE OF SIGNIFICANT POINTS		
	SST	PMSL	500 mb
JANUARY	15	18	13
FEBRUARY	13	21	20
MARCH	12	28	20
APRIL	13	30	19
MAY	12	34	30
JUNE	11	30	29
JULY	11	25	16
AUGUST	19	32	32
SEPTEMBER	18	28	14
OCTOBER	17	33	19
NOVEMBER	18	30	21
DECEMBER	15	14	13

Table 3 Percentage of data points which are significant when mean 1950-59 PMSL, SST or 500 mb Height data is subtracted from mean 1968-84 data for the month shown. See Figs 9 and 10 for geographical extent of data.

NOTE The percentages for PMSL are likely to have been exaggerated by inhomogeneities in the PMSL data set.

Table 4a Forecasts of Sahel rainfall (mainly July to September) from 1968 to 1985 using March to May SST EOF coefficients with training data from 1901-1967. The EOFs used were for 1901-80 and 1951-80

Year	Observed (1901-67 Quint Quints)	Forecast using 1901-80 EOFs	Forecast using 1951-80 EOFs
1968	1	5	3
1969	3	1	1
1970	1	1	2
1971	1	3	3
1972	1	1	1
1973	1	1	1
1974	1	3	2
1975	1	3	1
1976	1	1	1
1977	1	1	1
1978	2	1	2
1979	1	1	1
1980	1	1	1
1981	1	1	2
1982	1	1	1
1983	1	1	1
1984	1	3	1
1985	1	1	1
% Of correct forecasts (Hits) 61%			67%

Table 4b Probability forecasts of Sahel rainfall using a 1946-80 training period: predictors are March to May coefficients of 1951-80 eigenvectors. The average of the best 2 models are shown.

Year	Forecast Probabilities					Observed Quint.
	Quint 1	Quint 2	Quint 3	Quint 4	Quint 5	
1981	0.14	0.24	0.17	0.26	0.14	1
1982	0.51	0.34	0.02	0.06	0.07	1
1983	0.62	0.32	0.02	0.03	0.01	1
1984	0.46	0.35	0.06	0.09	0.04	1

(1946-80 Quints)

Table 4c Average of 9 forecasts for 1985 and 1986. All models are based on a 1946-84 training period and use predictors formed from 1951-80 EOFs. Models use April to May, March to May and March to April SST's as predictors: each produces a forecast based on 3, 4 and 5 variables, hence a total of 9 forecasts.

Year	Forecast Probabilities					Observed
	Quint 1	Quint 2	Quint 3	Quint 4	Quint 5	
1985	0.59	0.13	0.12	0.14	0.02	<b>2</b>
1986	0.27	0.53	0.14	0.05	0.01	1?

(1946-84 Quints)

1946-84 Quint Boundaries

		% standardised Units (1901-80)	(Fig 7a)
		Normal	
Quint 1	Quint 2	= 74	
Quint 2	Quint 3	- 37	
Quint 3	Quint 4	- 6	
Quint 4	Quint 5	+ 30	

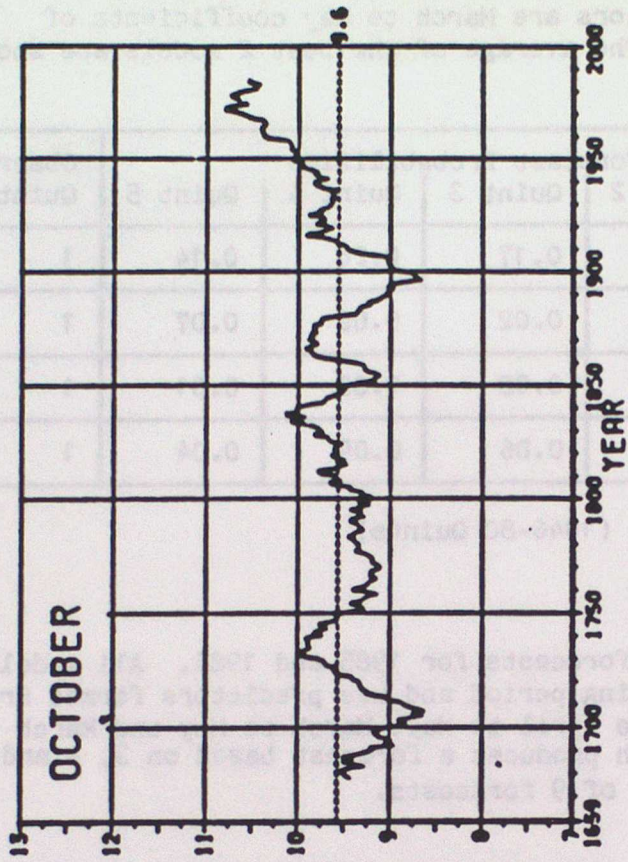
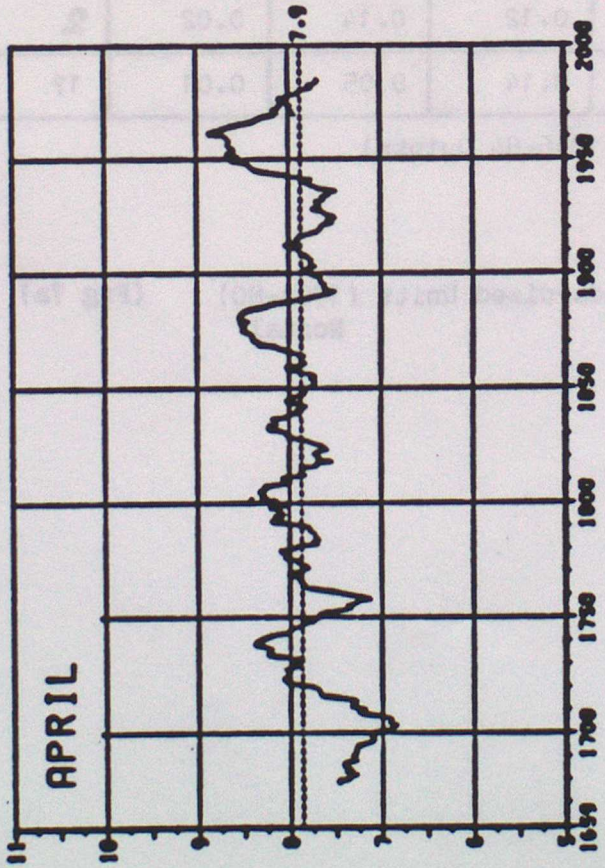


Figure 1 Long-term changes in Central England Temperature in April and October.

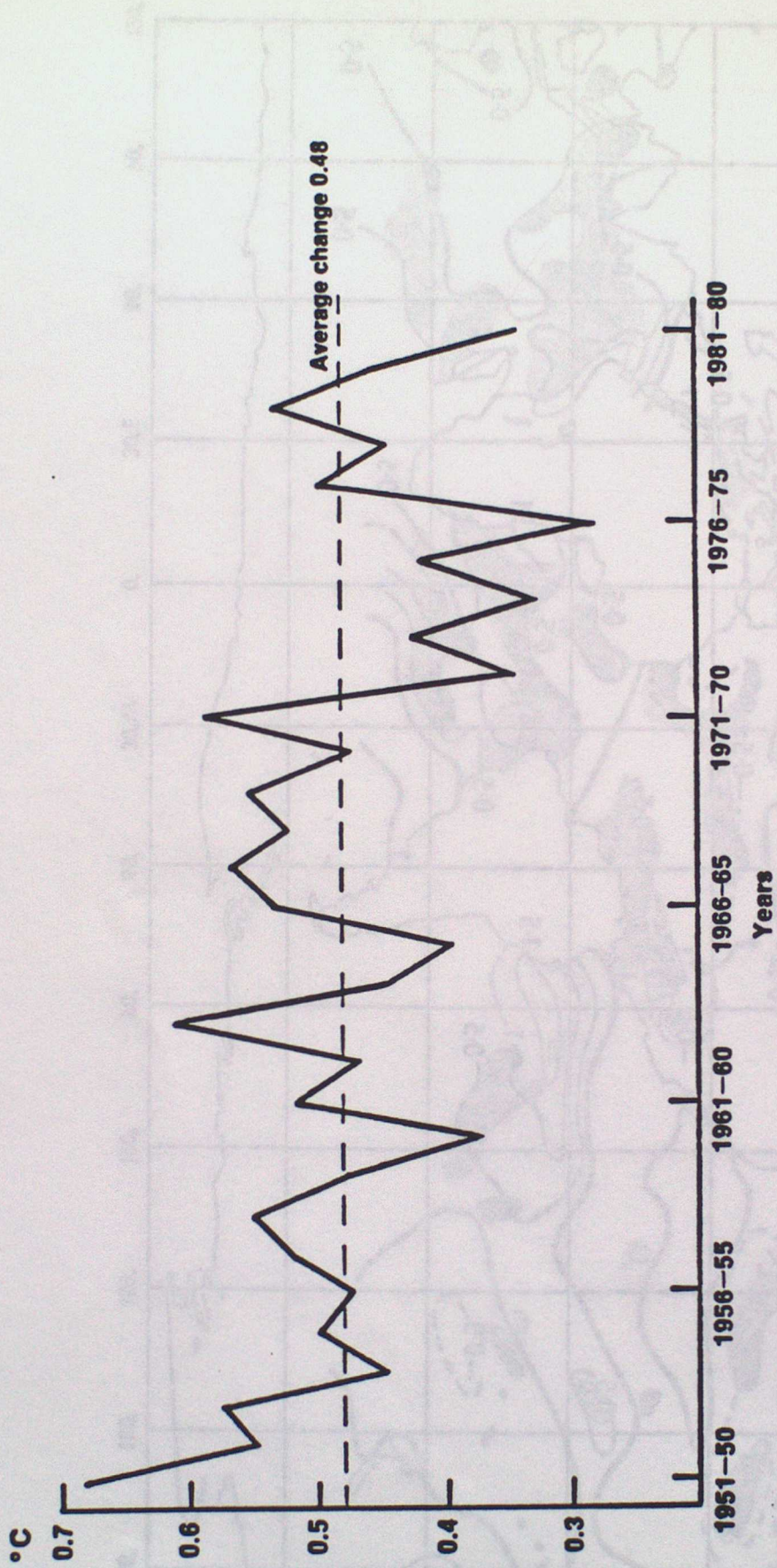


Figure 2 Mean modulus of interannual changes in combined July and August SST anomaly.  
 (Calculated on a  $20^\circ \times 20^\circ$  spatial scale).

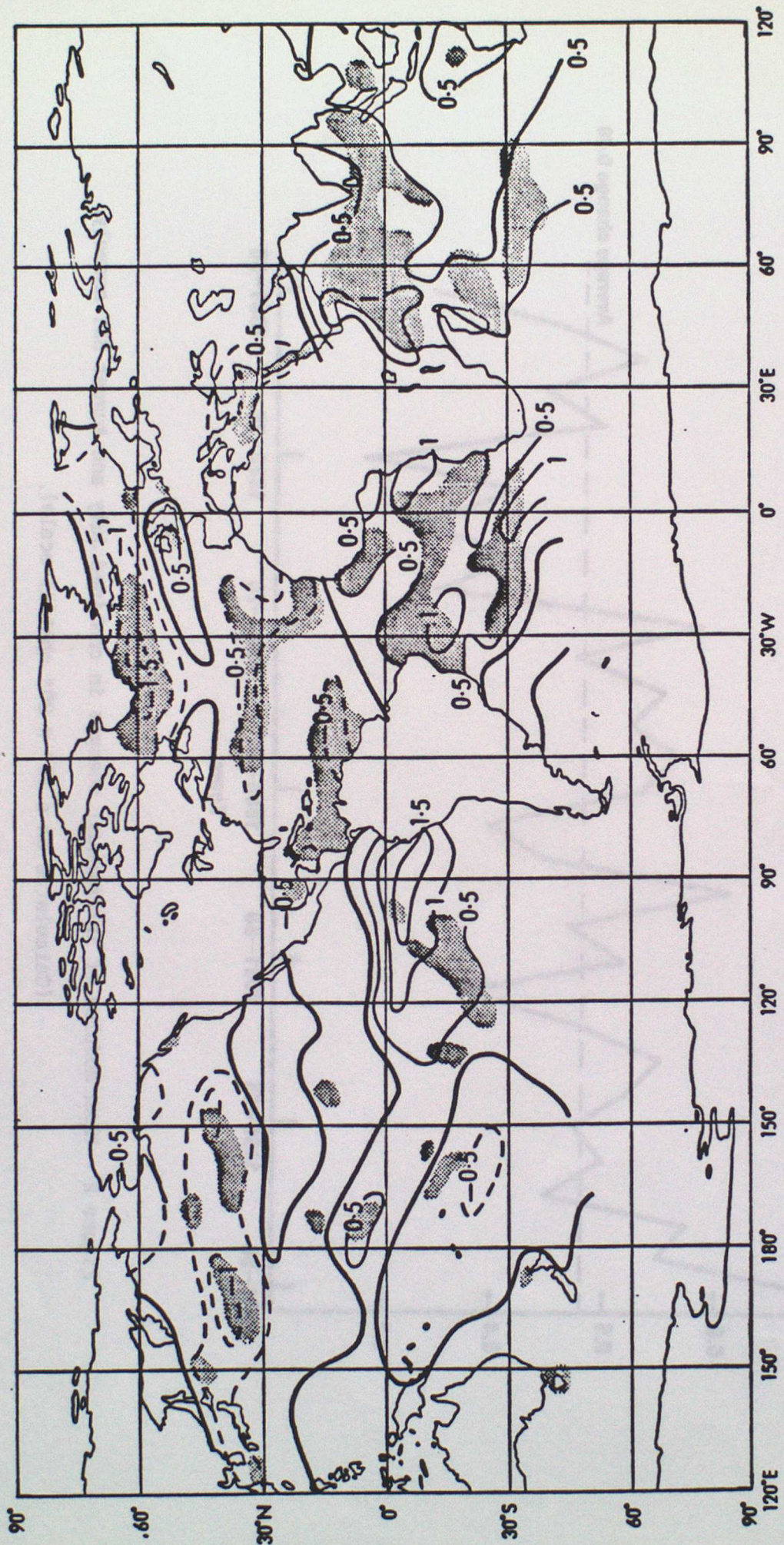


Figure 3 Difference in July to September SST between five driest and five wettest Sahel wet seasons (1950-1984)

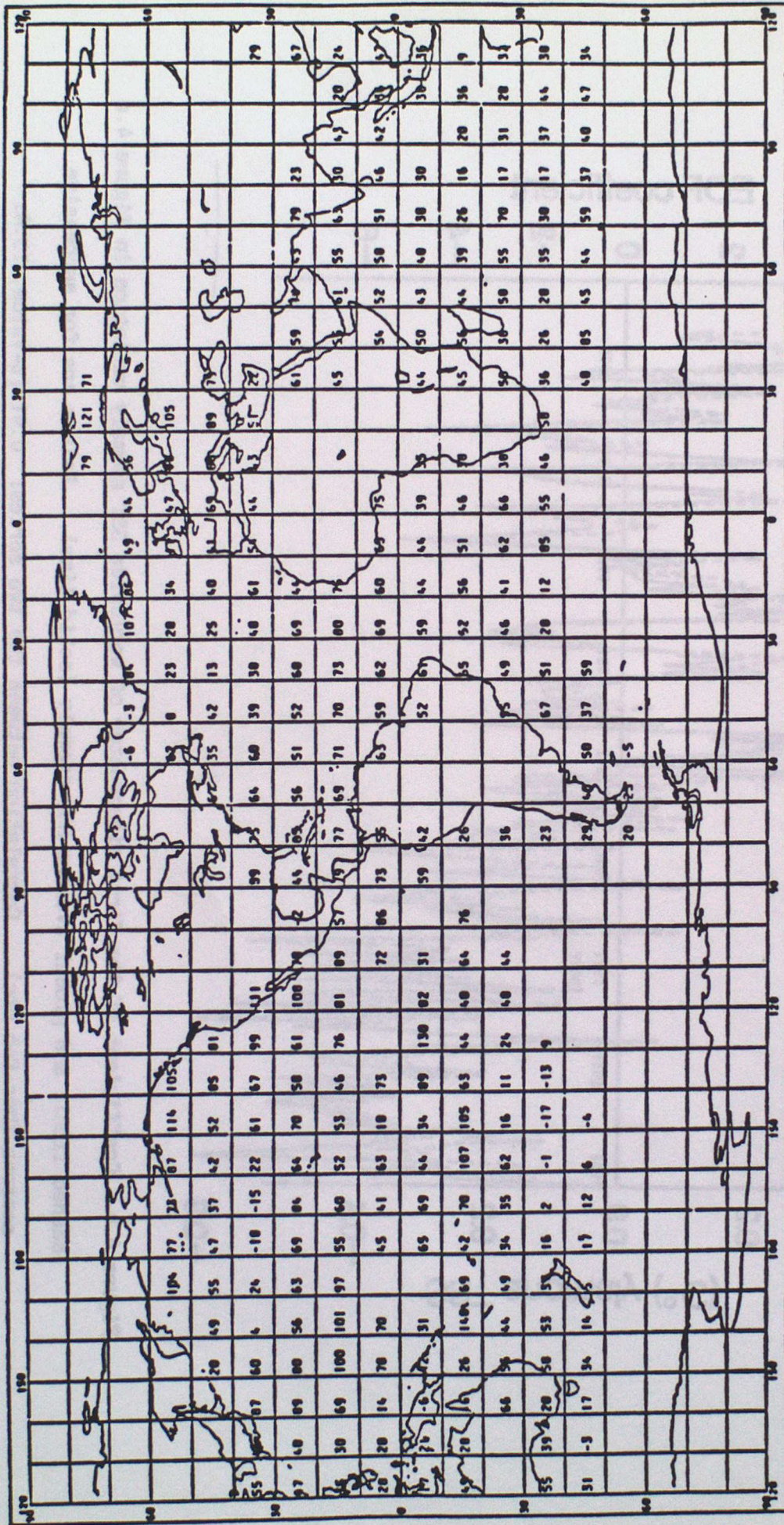


Figure 4.a First eigenvector of worldwide SST anomaly variation, 1901-1980

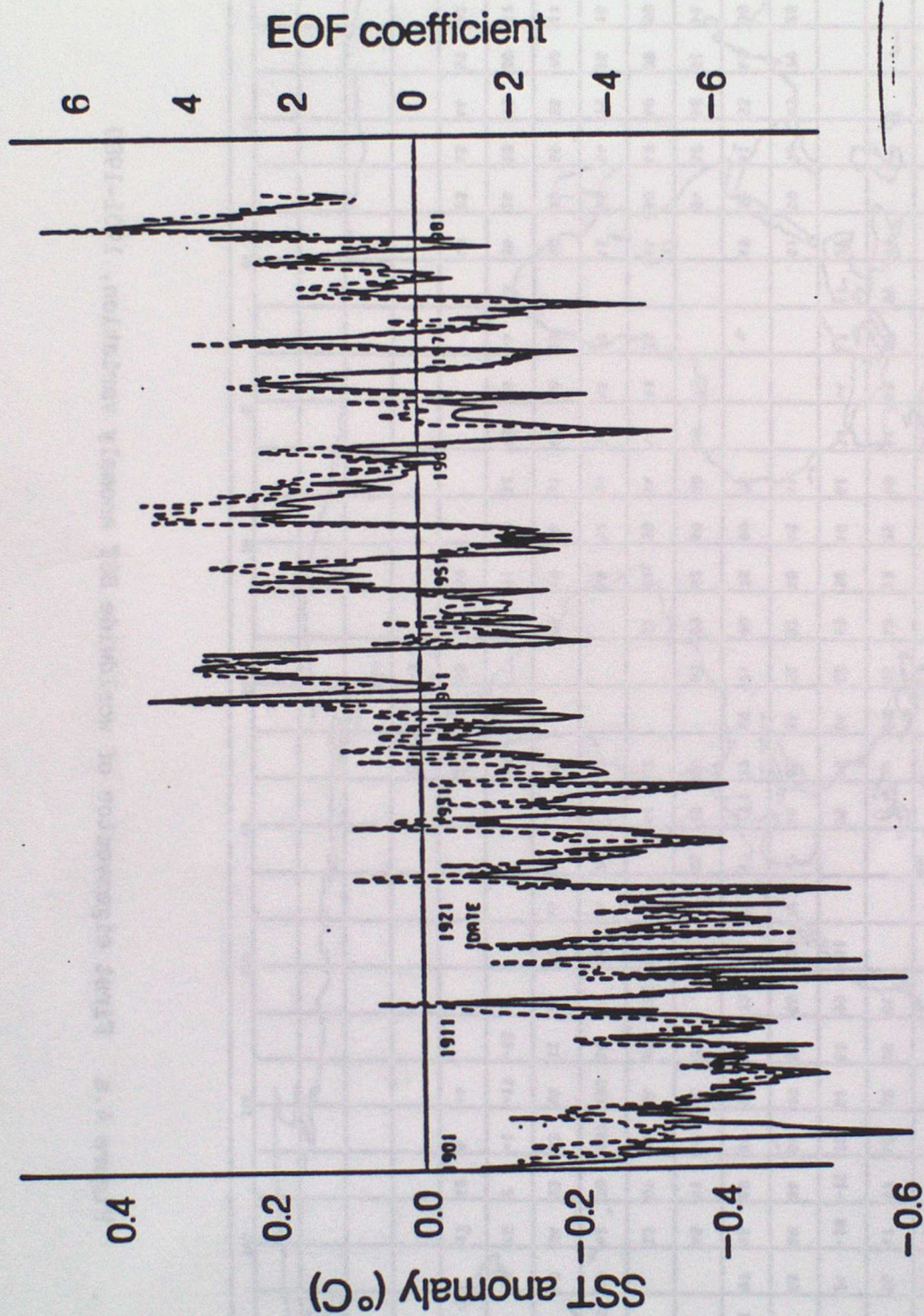


Figure 4.b Coefficient of the first eigenvector of worldwide SST anomaly variation in Figure 4.a (dashed line), and global average SST anomaly (solid line). Values are for successive seasons (Dec-Feb etc). Correlation between the two series: 0.91 (t-value, 13.8: significance  $\ll 10^{-8}\%$ )



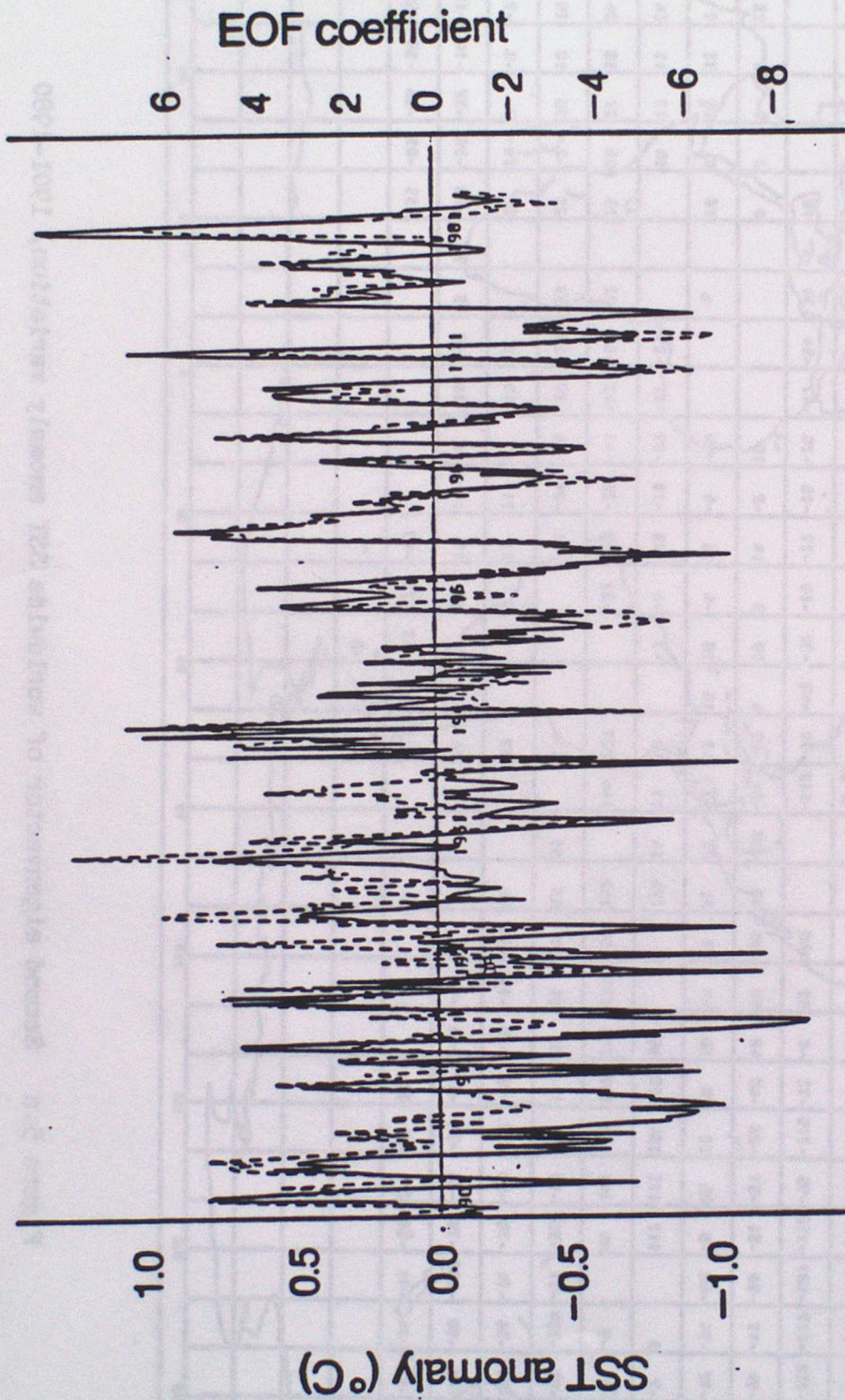


Figure 5.b Coefficient of the second eigenvector of worldwide SST anomaly variation in Figure 5.a (dashed line), and average SST anomaly in the E Tropical Pacific (20°N-20°S, east of 170°W) (solid line). Values are for successive seasons (Dec-Feb etc). Correlation between the two series: 0.65 (t-value, 5.4: significance  $2 \times 10^{-4}\%$ ) (EOF leads by one season)



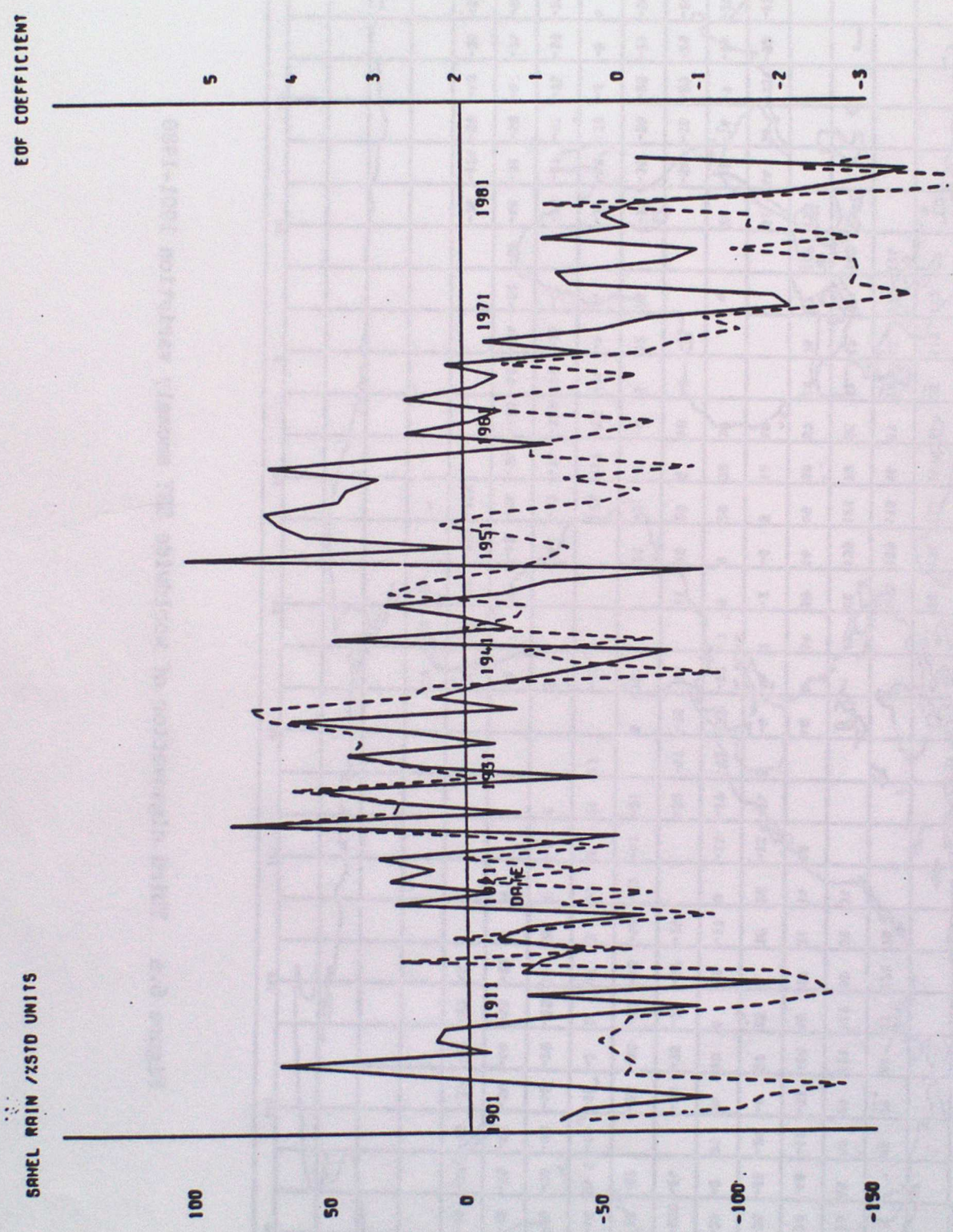


Figure 6.b Coefficient in June to August of the third eigenvector of worldwide SST anomaly variation in

Figure 6.a (dashed line), and Sahel rainfall (which falls mainly in July to September) (solid line).

Correlation between the two series: 0.60 (t-value, 4.75: significance,  $2 \times 10^{-3}\%$ ).

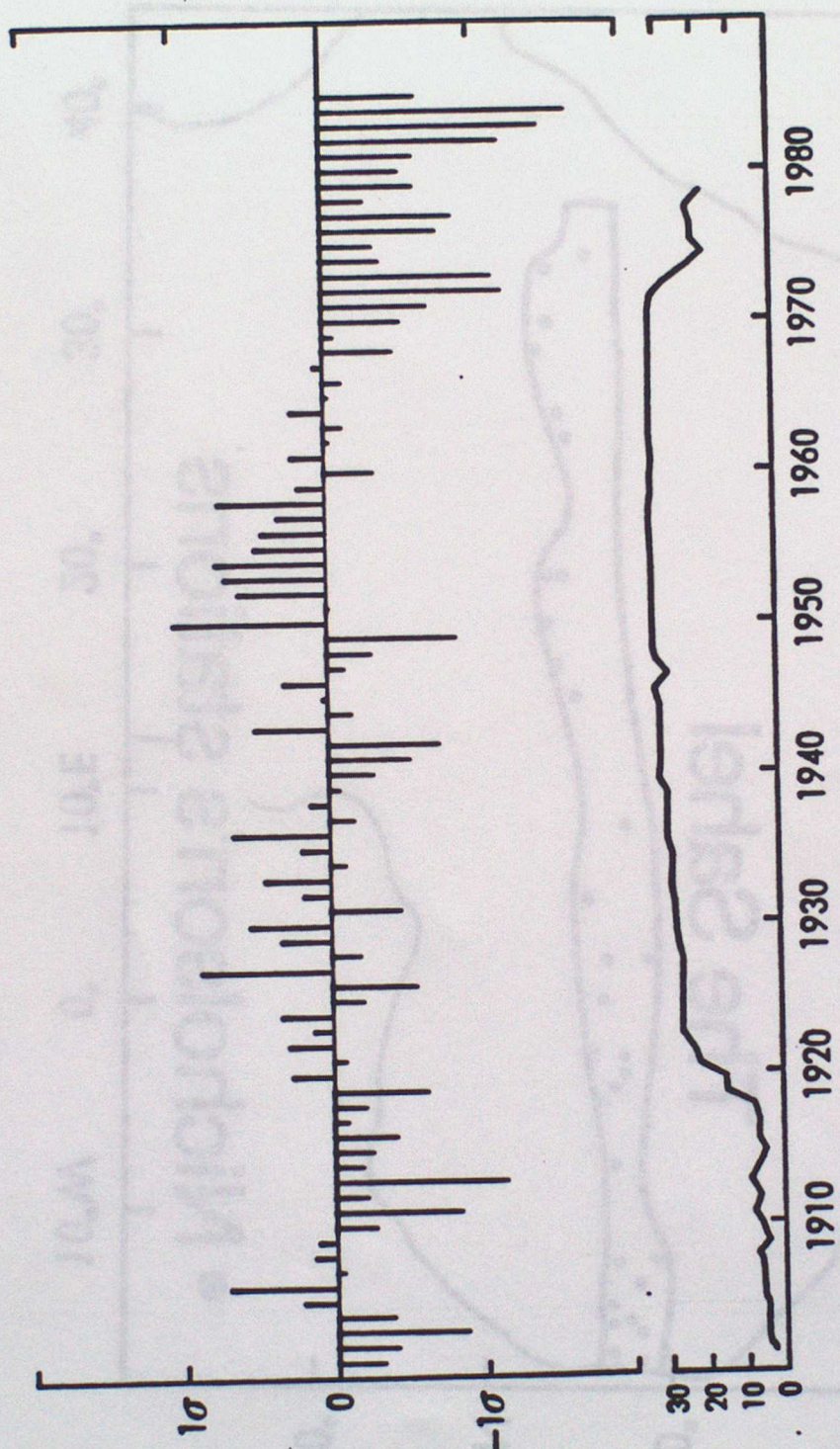


Figure 7.a Standardized annual rainfall anomalies for the Sahel, 1901-1985 (upper panel). Values to 1984 are after Nicholson (1985); 1985 values are from CLIMAT reports. The lower panel gives the number of stations used.

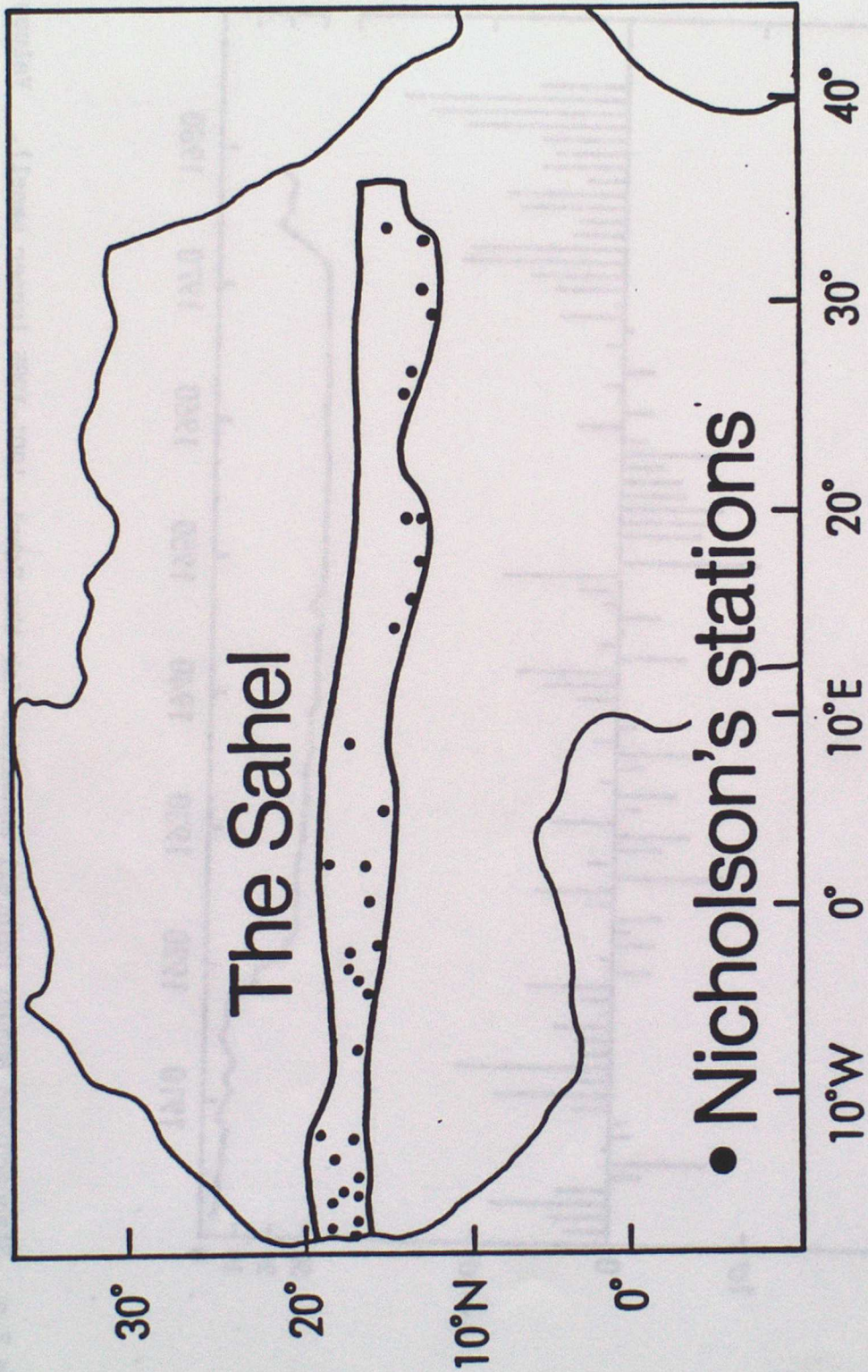


Figure 7.b Sahel rainfall stations used by Nicholson.

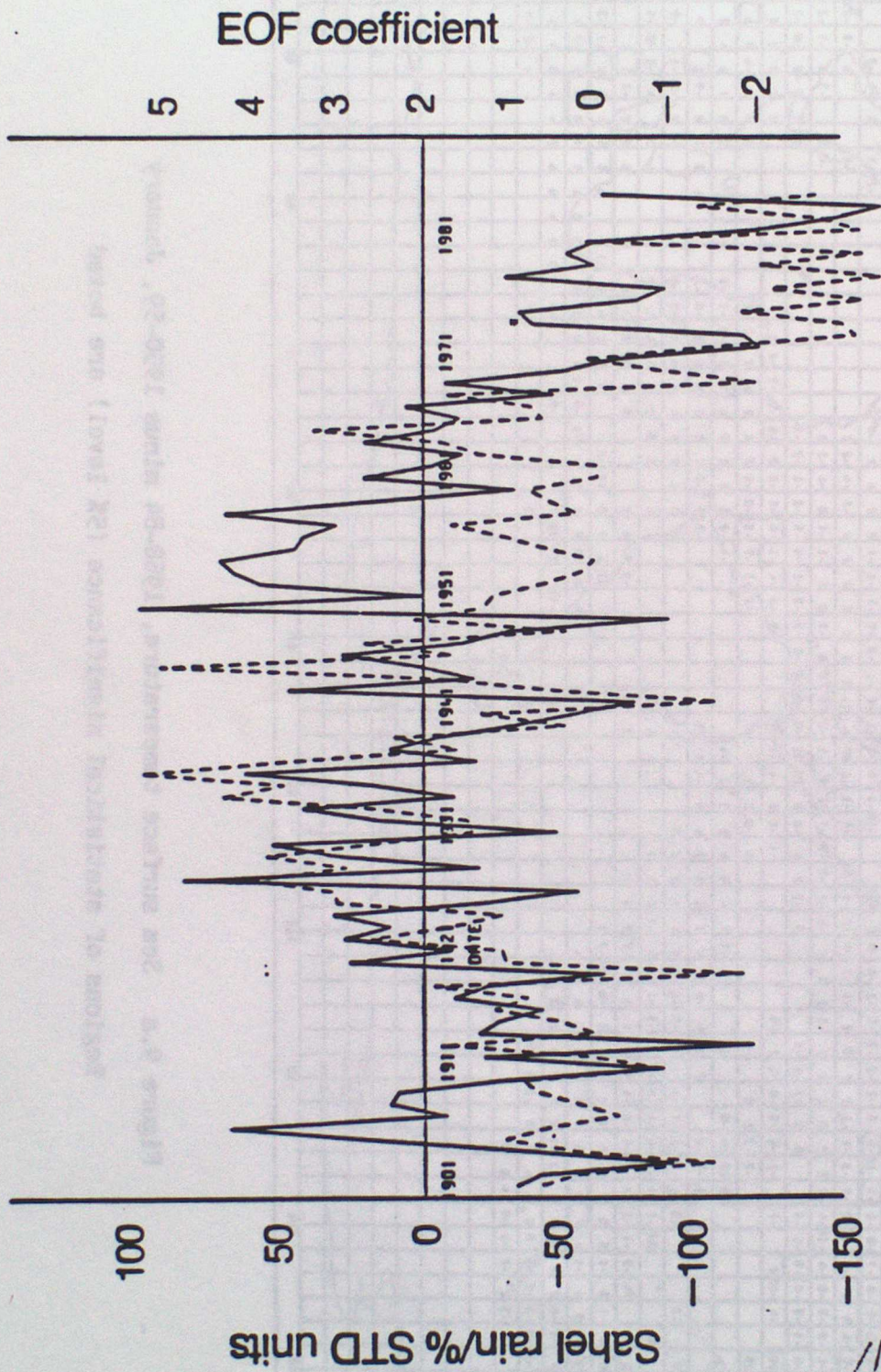


Figure 8 Coefficient in March to May of the third eigenvector of worldwide SST anomaly variation in Figure 6.a (dashed line), and Sahel rainfall (solid line). Correlation between the two series: 0.58 (t-value, 4.50: significance,  $3 \times 10^{-3}$ %)

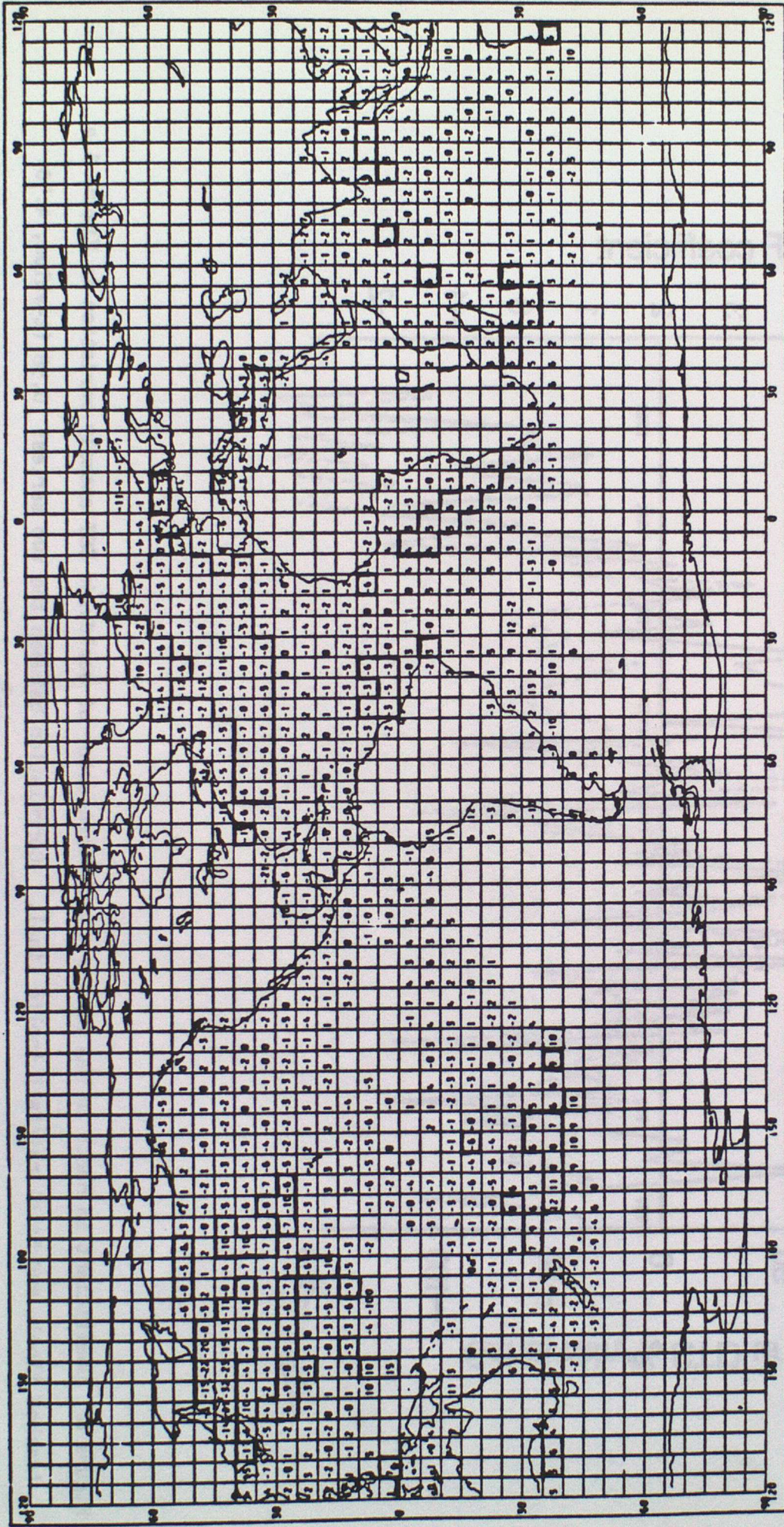


Figure 9.a Sea surface temperature, 1968-84 minus 1950-59, January  
Regions of statistical significance (5% level) are boxed

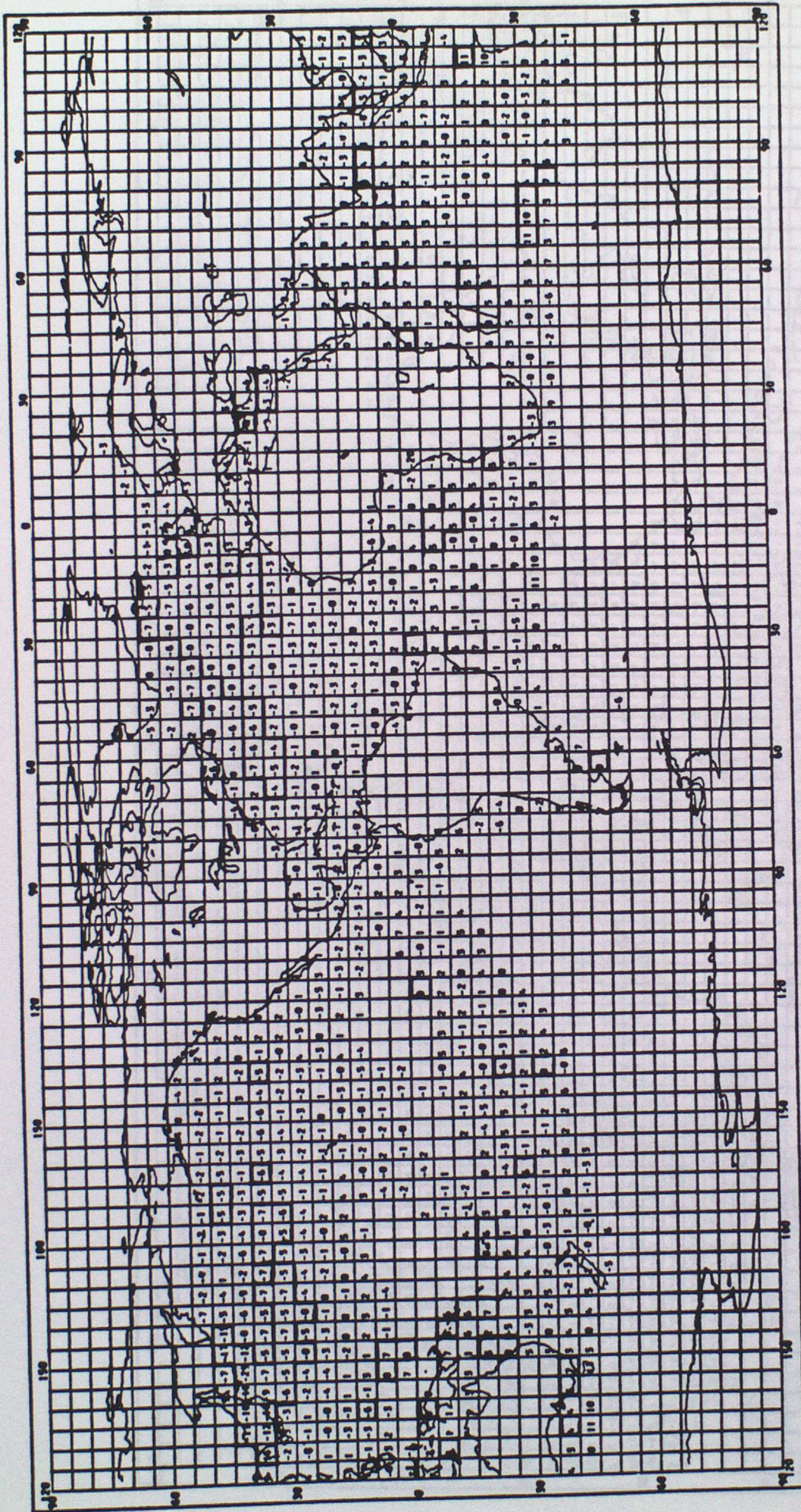
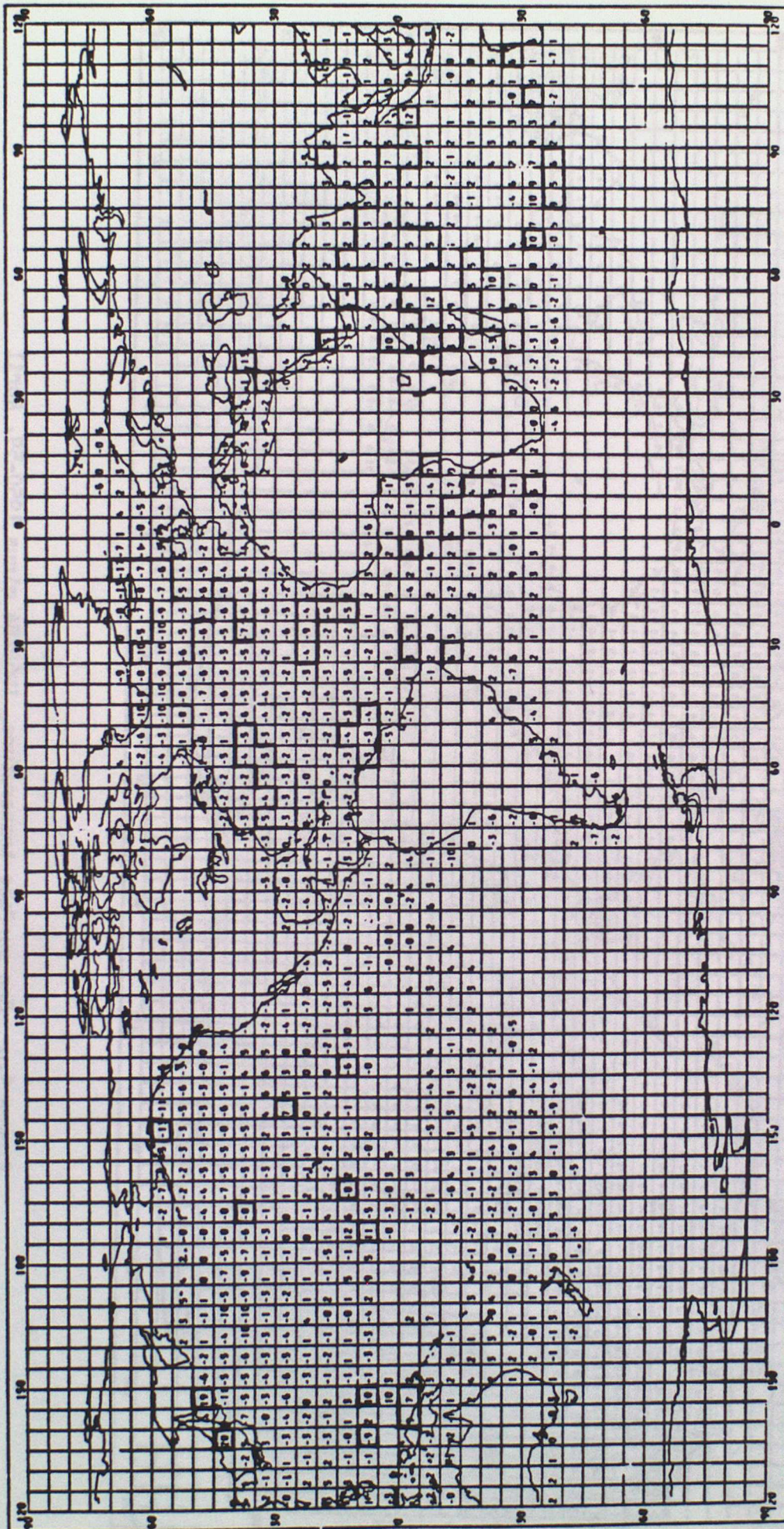


Figure 9.b Sea surface temperature, 1968-84 minus 1950-59, April

Regions of statistical significance (5% level) are boxed



• Figure 9.c Sea surface temperature, 1968-84 minus 1950-59, July  
 Regions of statistical significance (5% level) are boxed

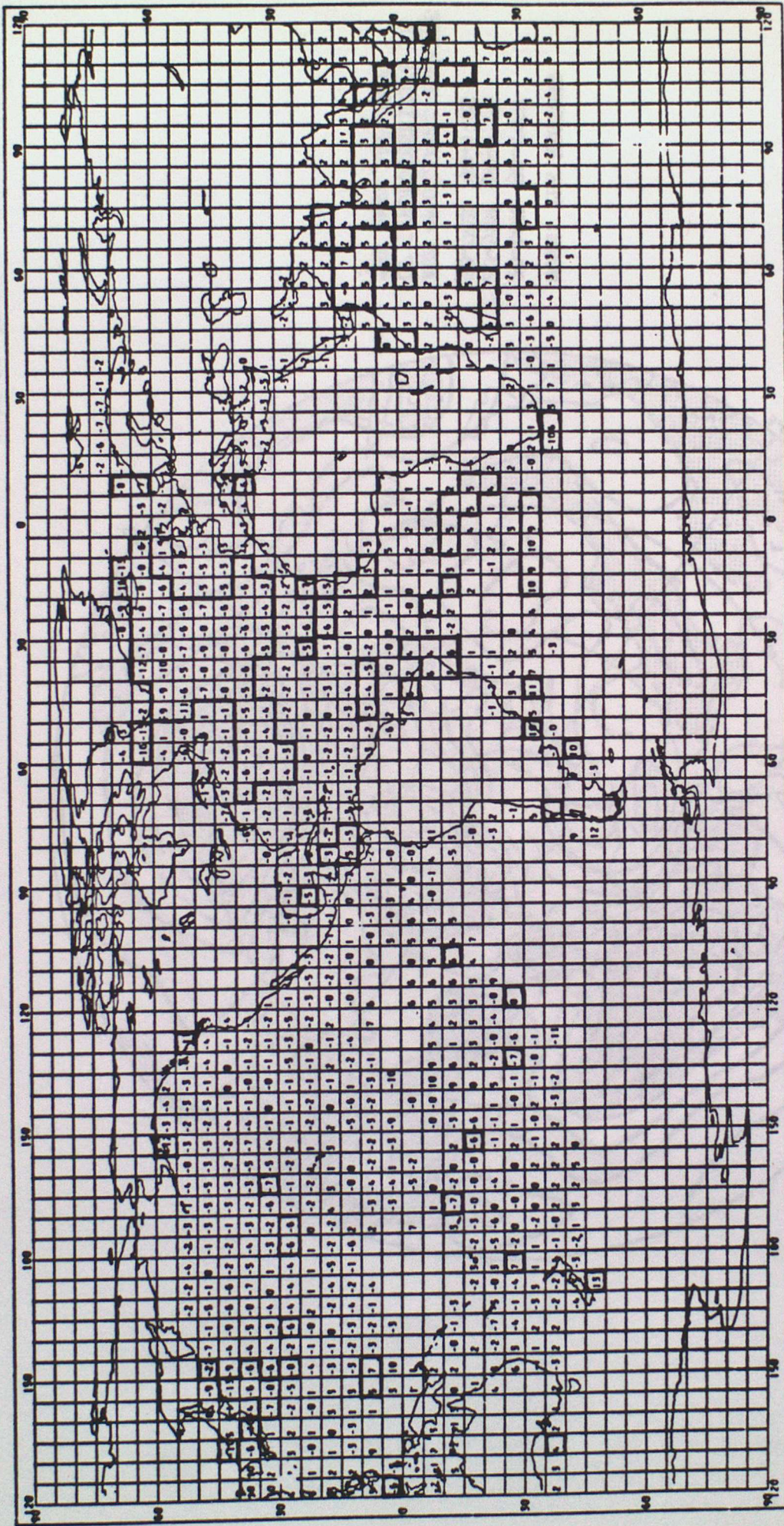


Figure 9.d Sea surface temperature, 1968-84 minus 1950-59, October  
 Regions of statistical significance (5% level) are boxed



NOTE: THE REGIONS

20-40N 90-115W

20-50N 50-130E

50-70N 90-140E

ARE UNRELIABLE BECAUSE  
OF INHOMOGENEITIES IN  
THE PMSL DATA SET

Figure 10.a MSL Pressure, extratropical N Hemisphere, 1968-84 minus 1950-59, March

Regions of statistical significance (5% level) are shaded

NOTE: THE REGIONS  
 20-40N 90-115W  
 20-50N 50-130E  
 50-70N 90-140E  
 ARE UNRELIABLE BECAUSE  
 OF INHOMOGENEITIES IN  
 THE PMSL DATA SET

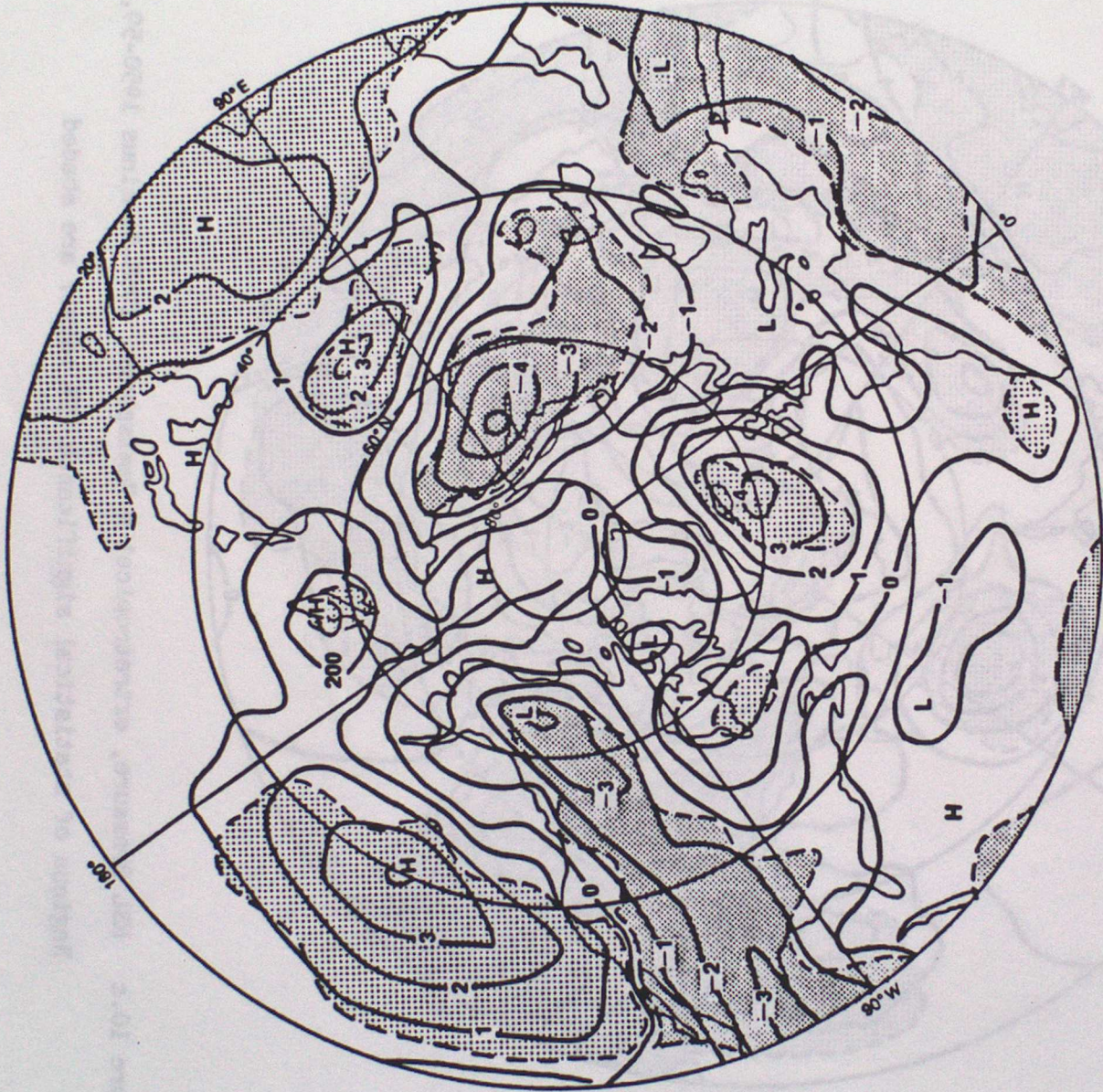
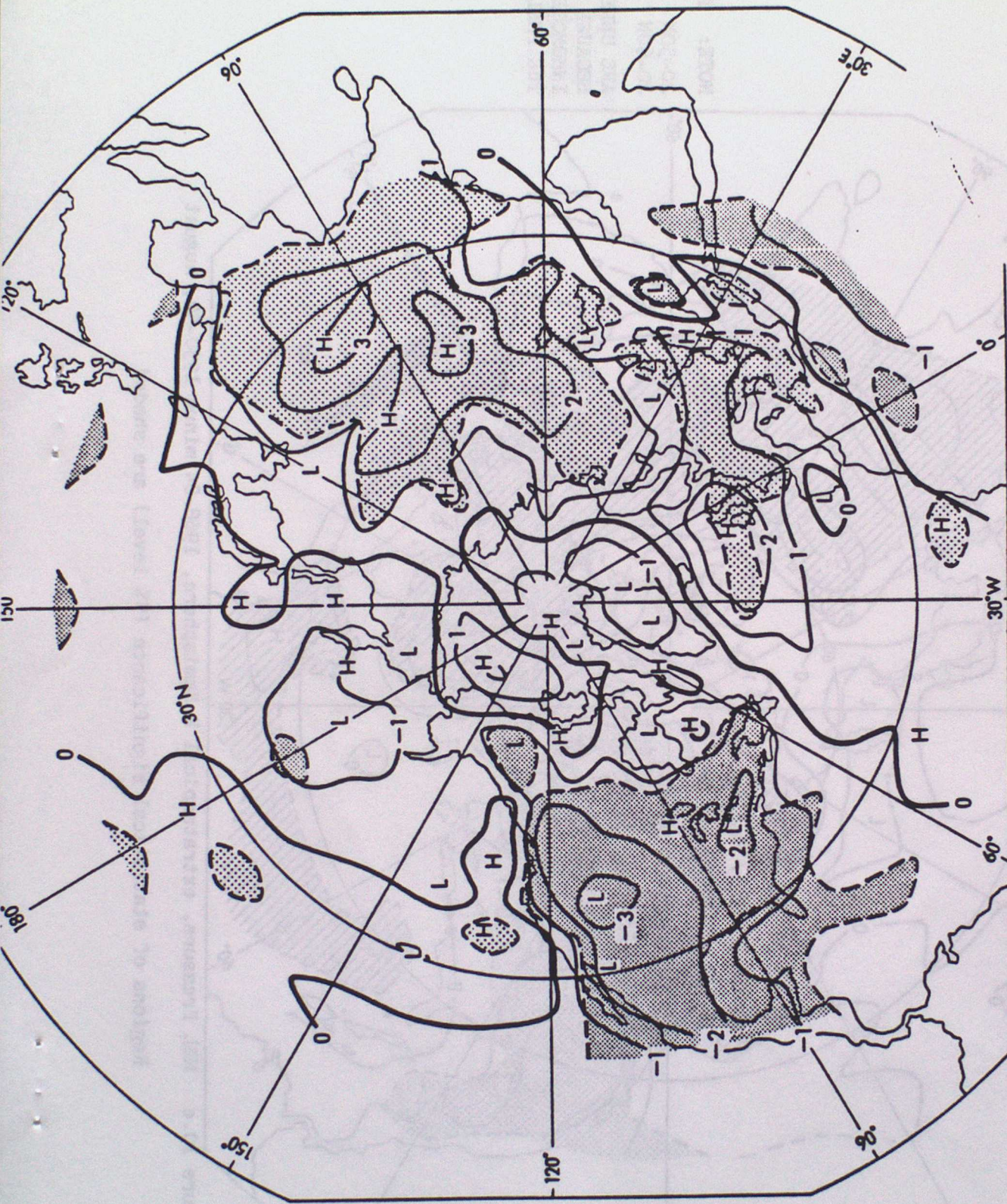


Figure 10.b MSL Pressure, extratropical N Hemisphere, 1968-84 minus 1950-59, April  
 Regions of statistical significance (5% level) are shaded

NOTE: THE REGIONS  
20-50N 90-120W  
20-60N 60-130E  
ARE UNRELIABLE BECAUSE  
OF INHOMOGENEITIES IN  
THE PMSL DATA SET



Figure 10.c MSL Pressure, extratropical N Hemisphere, 1968-84 minus 1950-59, May  
Regions of statistical significance (5% level) are shaded



NOTE: THE REGIONS  
 20-50N 90-120W  
 20-60N 60-130E  
 ARE UNRELIABLE BECAUSE  
 OF INHOMOGENEITIES IN  
 THE PMSL DATA SET

Figure 10.d MSL Pressure, extratropical N Hemisphere, 1968-84 minus 1950-59, July

Regions of statistical significance (5% level) are shaded

NOTE: THE REGIONS  
 20-50N 90-120W  
 20-60N 60-130E  
 ARE UNRELIABLE  
 BECAUSE OF  
 INHOMOGENEITIES IN  
 THE PMSL DATA SET

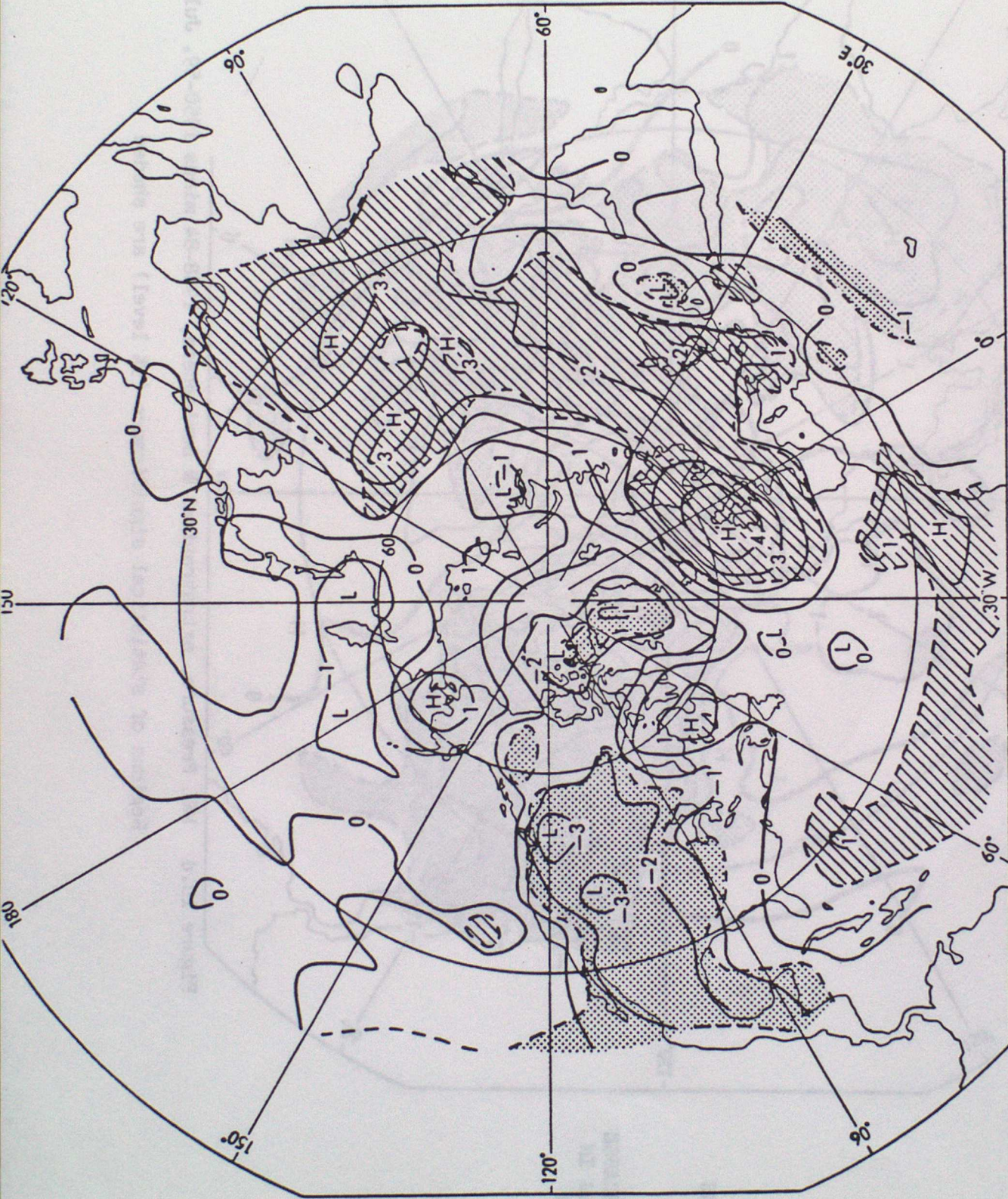


Figure 10.e MSL Pressure, extratropical N Hemisphere, 1968-84 minus 1950-59, August

Regions of statistical significance (5% level) are shaded

NOTE: THE REGIONS  
 20-45N 100-120W  
 20-50N 50-130E  
 50-70N 90-140E  
 ARE UNRELIABLE BECAUSE  
 OF INHOMOGENEITIES IN  
 THE PMSL DATA SET



Figure 10.f MSL Pressure, extratropical N Hemisphere, 1968-84 minus 1950-59, October  
 Regions of statistical significance (5% level) are shaded



NOTE: THE REGIONS

20-40N 90-115W

20-50N 50-130E

50-70N 90-140E

ARE UNRELIABLE BECAUSE  
OF INHOMOGENEITIES IN  
THE PMSL DATA SET

Figure 11.a MSL Pressure, extratropical N Hemisphere, 1968-84 minus 1950-59, December to March

Regions of statistical significance (5% level) are shaded

NOTE: THE REGIONS  
 20-50N 90-120W  
 20-60N 60-130E  
 ARE UNRELIABLE BECAUSE  
 OF INHOMOGENEITIES IN  
 THE PMSL DATA SET



Figure 11.b MSL Pressure, extratropical N Hemisphere, 1968-84 minus 1950-59, April to November  
 Regions of statistical significance (5% level) are shaded

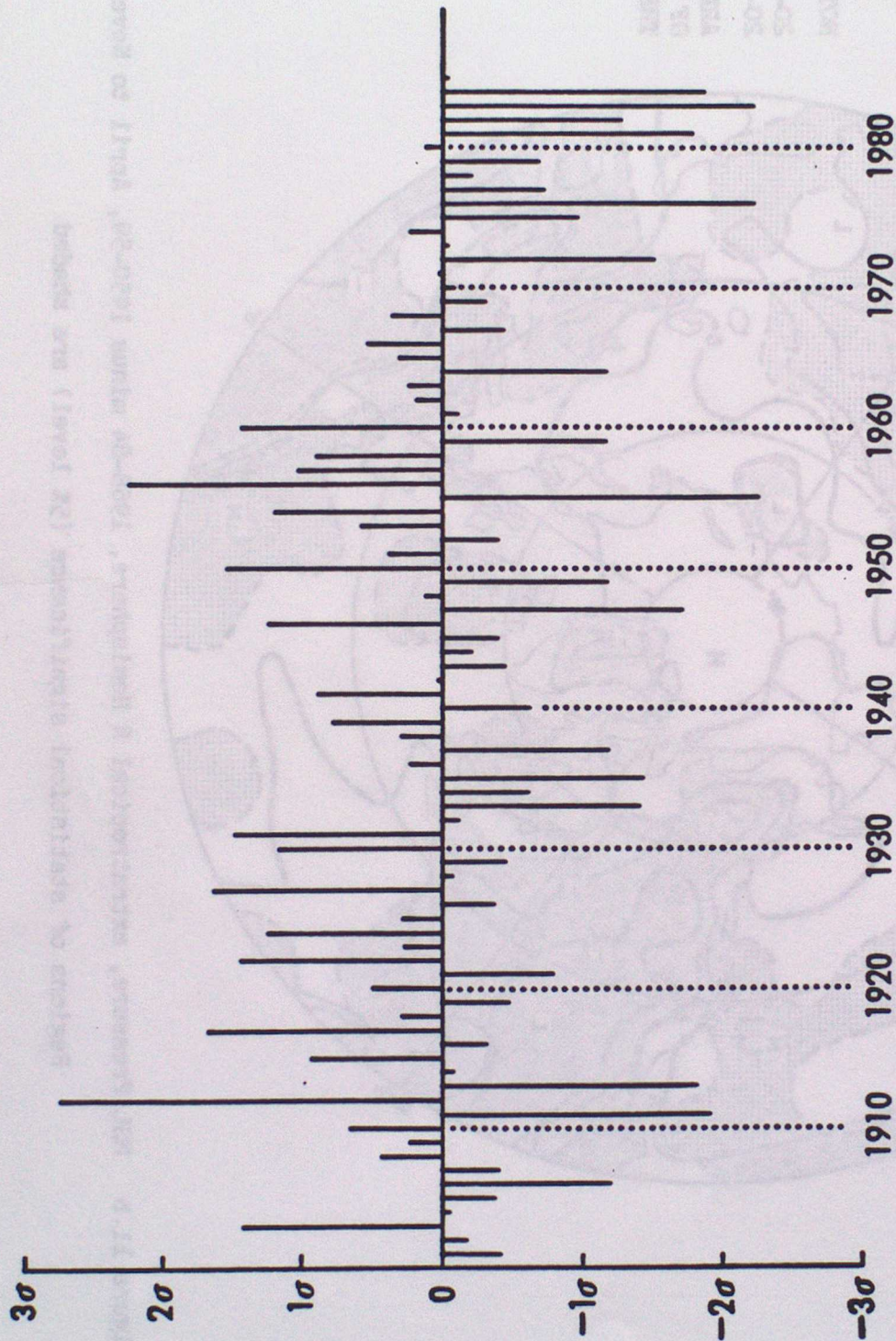


Figure 12 Standardised England and Wales July and August rainfall, 1901-85

USE THIS COPY FOR  
 THE INFORMATION ONLY BY  
 THE INFORMATION SERVICES  
 SD-200 00-1000  
 SD-200 00-1000  
 MAKE: AND MAKE

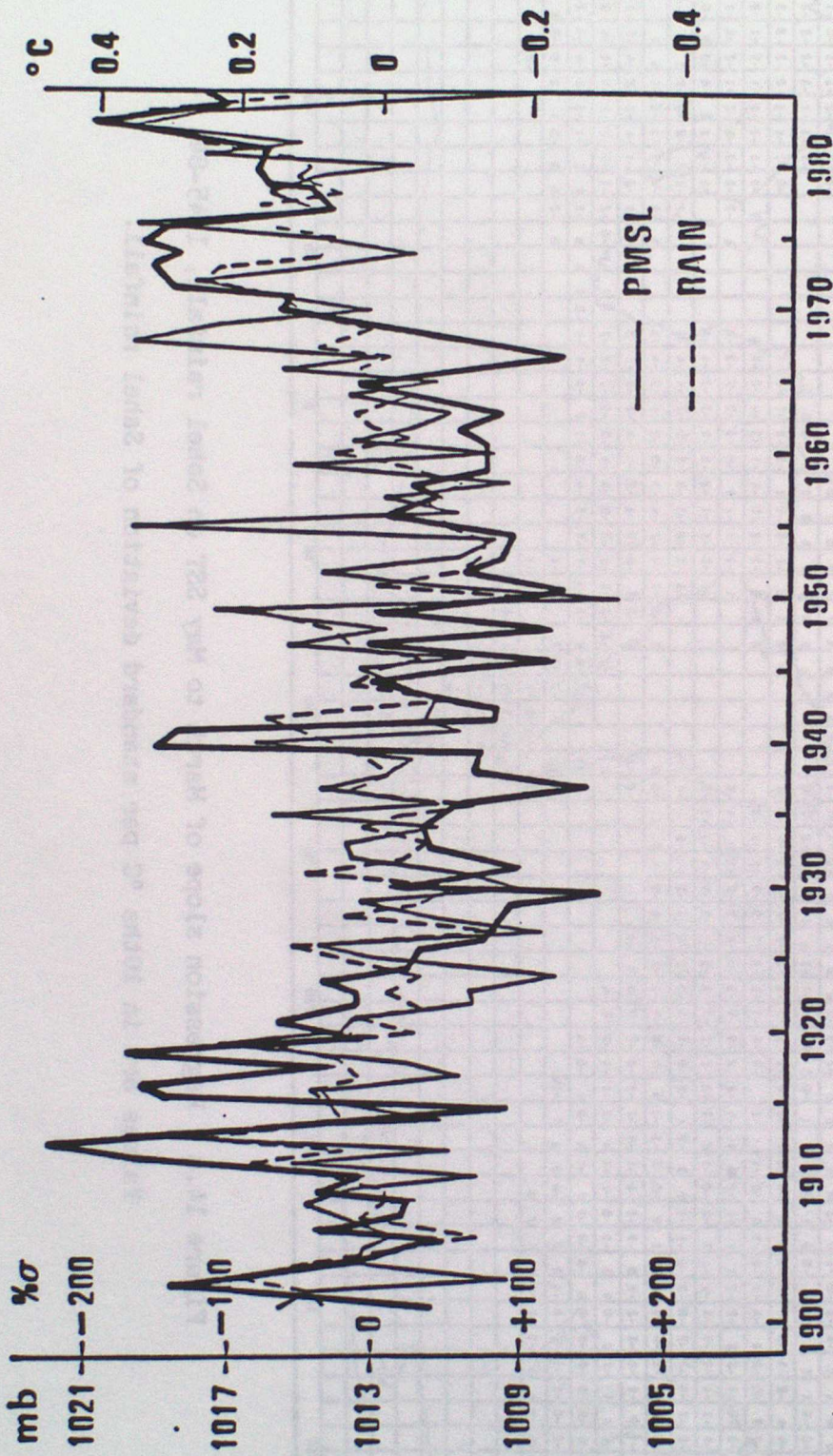


Figure 13.1 Mean MSL pressure at 55°N 10°W in July and August (—)

11 Annual Sahel rainfall (-----)

111 July to September SST, S Hemisphere with N Indian Ocean minus rest of N Hemisphere (—)

Correlations between series:

1.	vs 11):	0.29
1.	vs 111):	-0.53
11.	vs 111):	-0.63

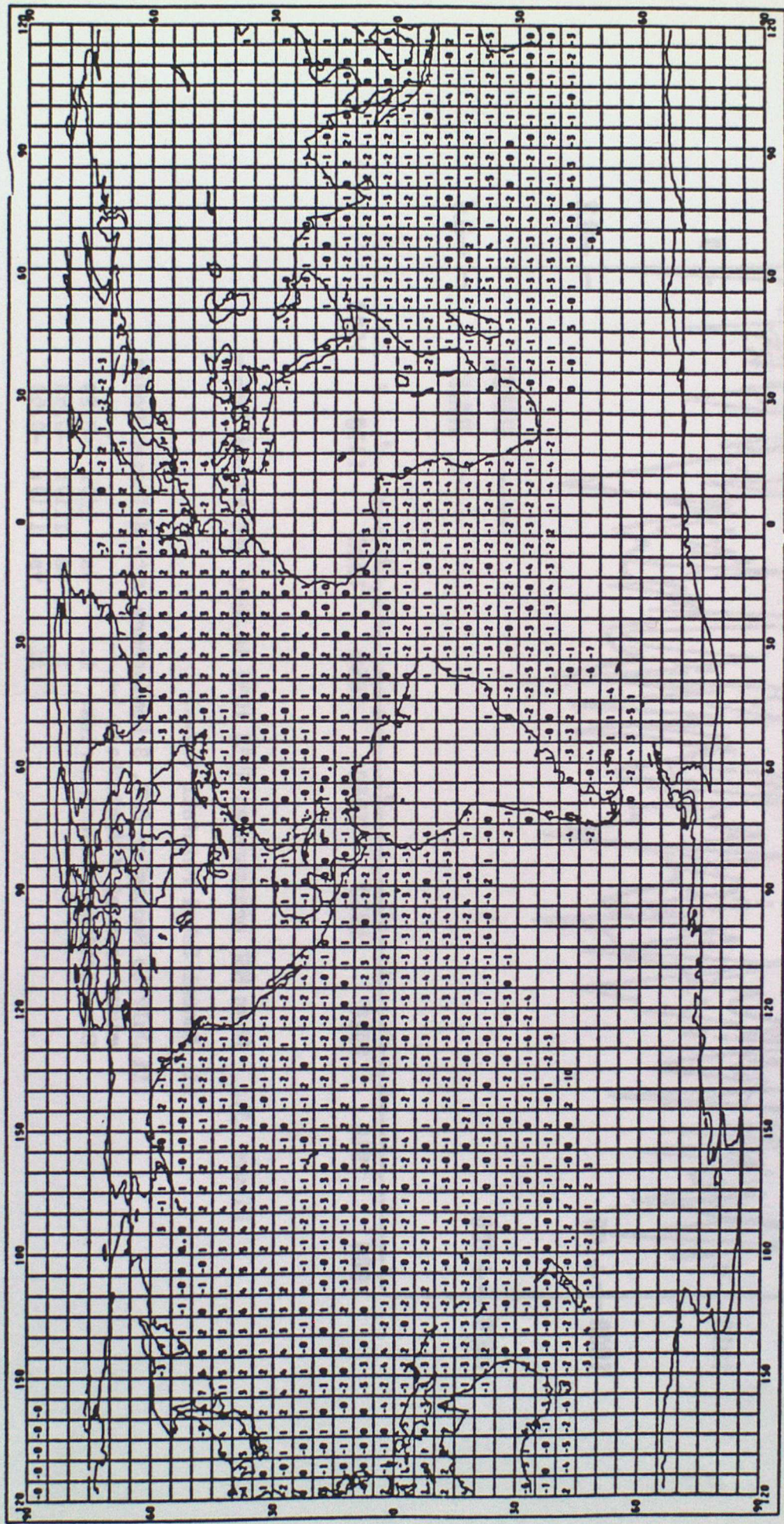


Figure 14.a Regression slope of March to May SST on Sahel rainfall, 1945-84.

Values are in 10ths °C per standard deviation of Sahel rainfall.

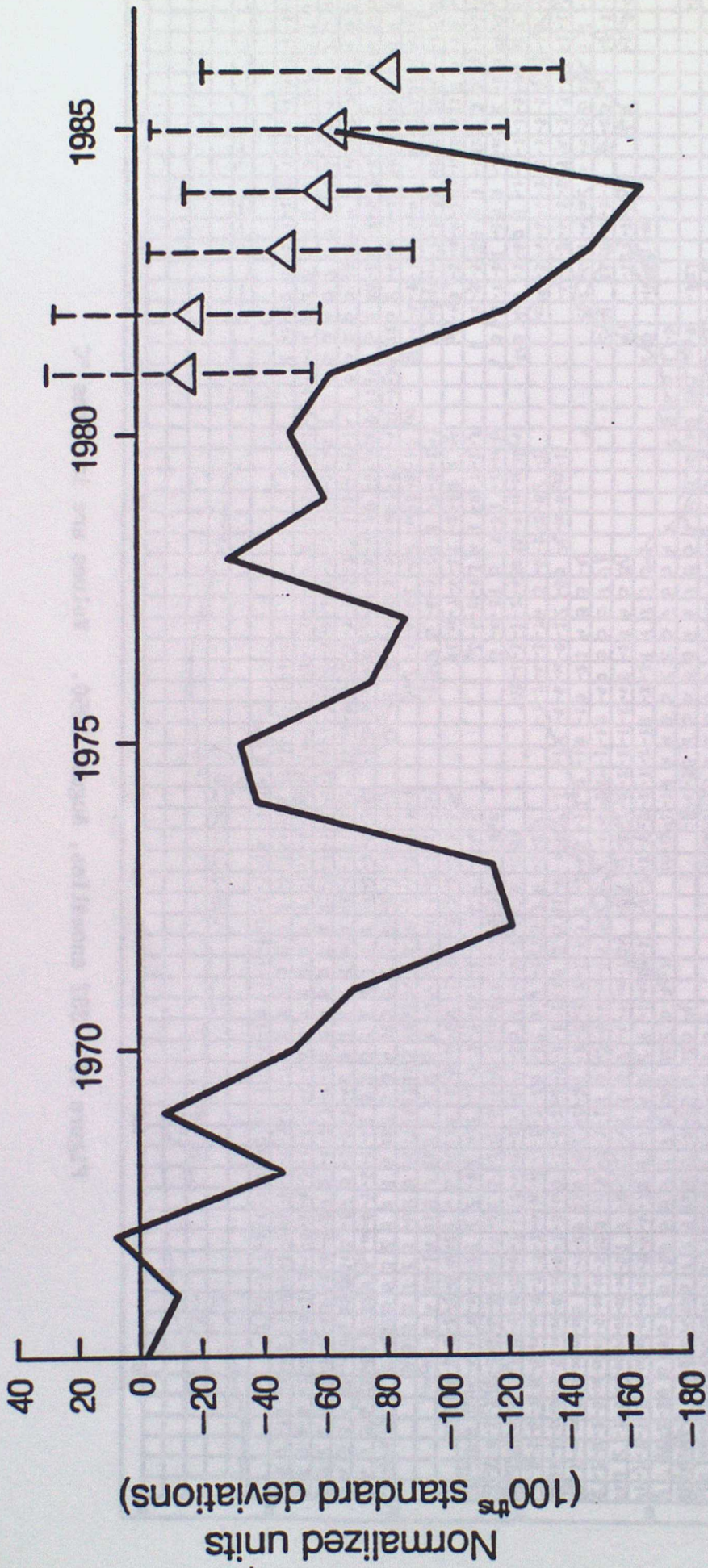


Figure 14.b Observed Sahel rainfall, 1965-85; and predicted values, 1981-6, using regression technique.

The bars on the predictions give the 95% confidence limits.

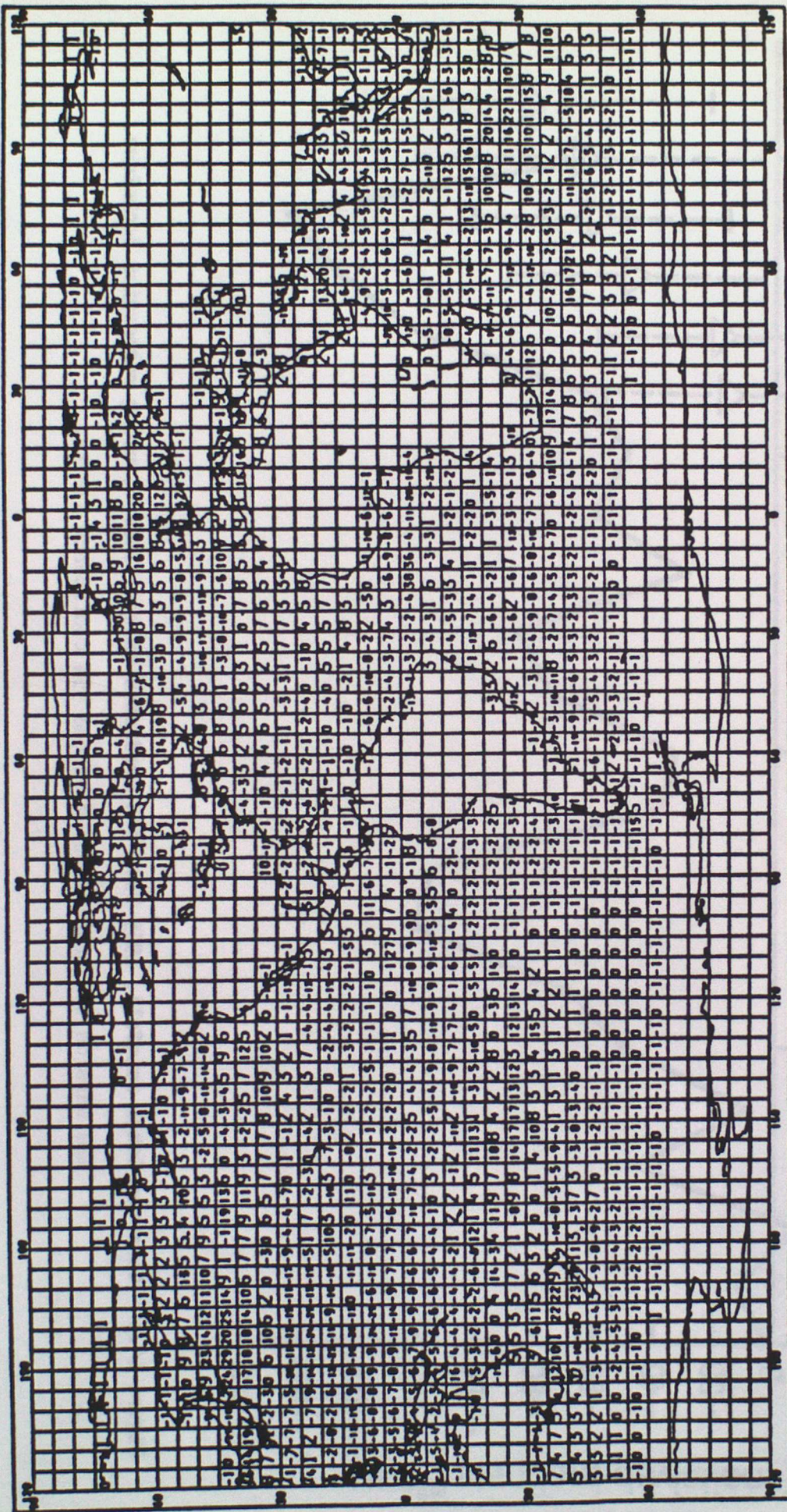


Figure 15 SST anomalies, August 1950. Values are in 10ths °C

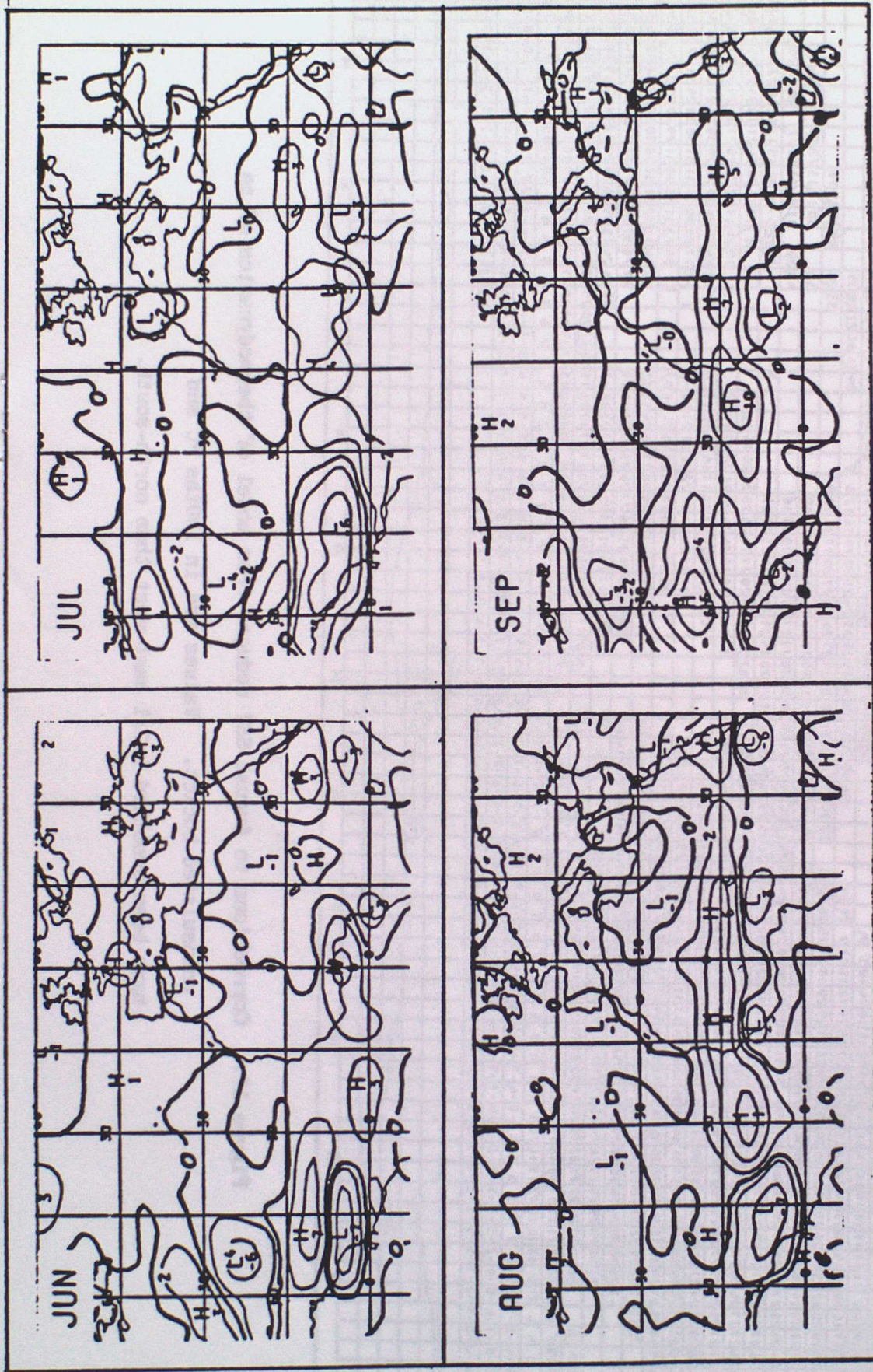


Figure 16. Monthly deviations of rainfall (mm) from climatology of numerical general circulation model forced by SST anomalies for 1950.

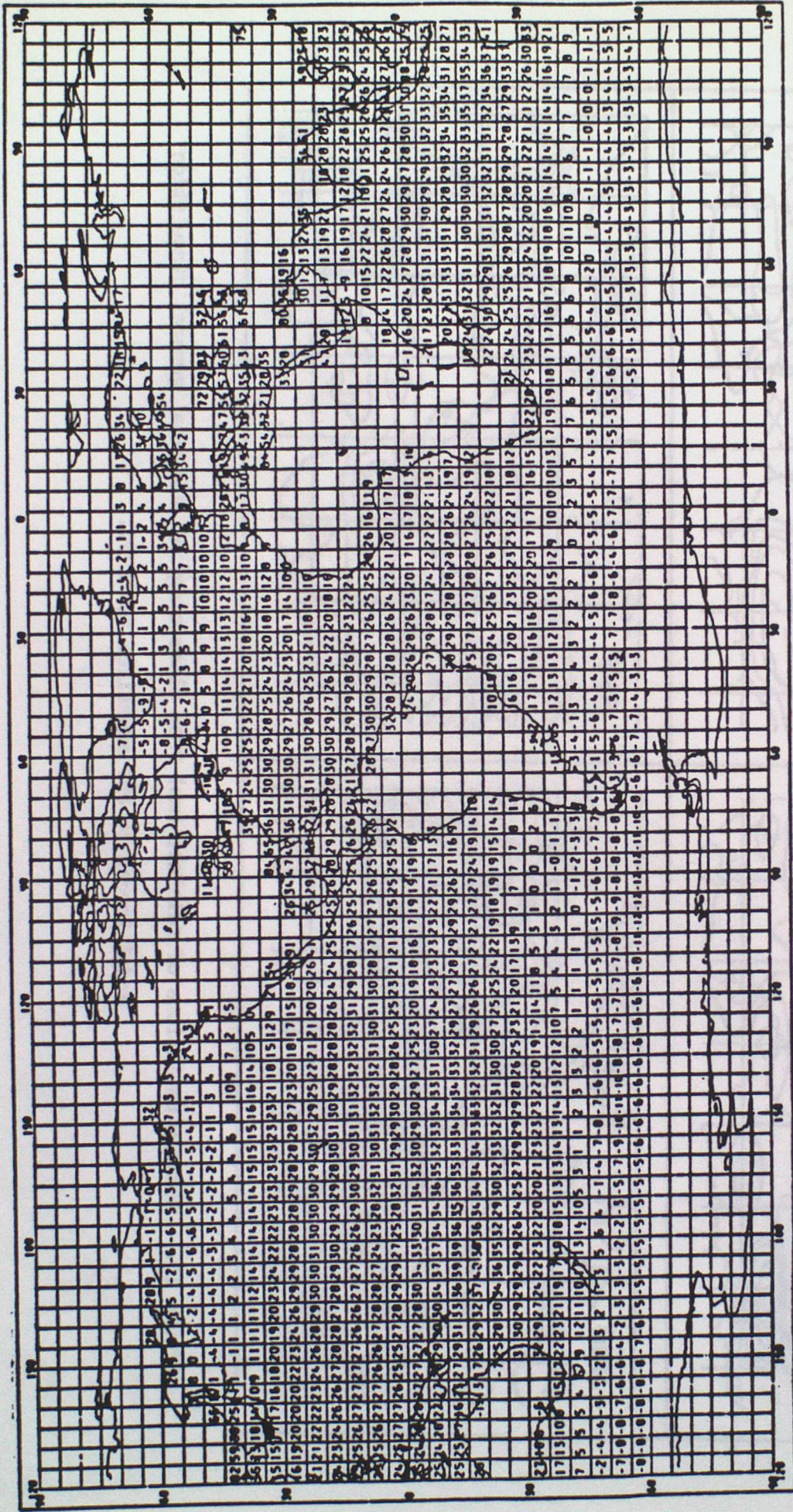


Figure 17. Corrections to August SST deduced from model of thermodynamics of an uninsulated bucket. Values are in 100ths °C and have been smoothed 1:2:1 east-west then north-south.

INDEX TO LONG-RANGE FORECASTING AND CLIMATE RESEARCH SERIES

- 1) THE CLIMATE OF THE WORLD - Introduction and description of world climate.  
by C K Folland (March 1986)
- 2) THE CLIMATE OF THE WORLD - Forcing and feedback processes.  
by C K Folland (March 1986)
- 3) THE CLIMATE OF THE WORLD - El Nino/Southern Oscillation and the Quasi-  
biennial Oscillation.  
by C K Folland (March 1986)
- 4) THE CLIMATE OF THE WORLD - Climate change: the ancient earth to the  
'Little Ice Age'.  
by C K Folland
- 5) THE CLIMATE OF THE WORLD - Climate change: the instrumental period.  
by C K Folland (March 1986)
- 6) THE CLIMATE OF THE WORLD - Carbon dioxide and climate (with appendix on  
simple climate models).  
by C K Folland (March 1986)
- 7a) Sahel rainfall, Northern Hemisphere circulation anomalies and worldwide sea  
temperature changes, (To be published in the Proceedings of the "Pontifical  
Academy of Sciences Study Week", Vatican, 23-27 September 1986).  
by C K Folland, D E Parker, M W Ward and A W Colman (September 1986)  
(Amended July 1987)
- 8) Lagged-average forecast experiments with a 5-level general circulation  
model.  
by J M Murphy (March 1986)
- 9) Statistical Aspects of Ensemble Forecasts.  
by J M Murphy (July 1986)
- 10) The impact of El Nino on an Ensemble of Extended-Range Forecasts.  
(Submitted to Monthly Weather Review)  
by J A Owen and T N Palmer (December 1986)
- 11) An experimental forecast of the 1987 rainfall in the Northern Nordeste  
region of Brazil.  
by M W Ward, S Brooks and C K Folland (March 1987)
- 12) The sensitivity of Estimates of Trends of Global and Hemispheric Marine  
Temperature to Limitations in Geographical Coverage.  
by D E Parker (April 1987)
- 13) General circulation model simulations using cloud distributions from the  
GAPOD satellite data archive and other sources.  
by R Swinbank (May 1987)

- 14) Simulation of the Madden and Julian Oscillation in GCM Experiments.  
by R Swinbank (May 1987)
- 15) Numerical simulation of seasonal Sahel rainfall in four past years  
using observed sea surface temperatures.  
by J A Owen, C K Folland and M Bottomley  
(April 1988)
- 16) Not used
- 17) A note on the use of Voluntary Observing Fleet Data to estimate air-sea  
fluxes.  
by D E Parker (April 1988)
- 18) Extended-range prediction experiments using an 11-level GCM  
by J M Murphy and A Dickinson (April 1988)
- 19) Numerical models of the Raingauge Exposure problems - field experiments  
and an improved collector design.  
by C K Folland (May 1988)
- 20) An interim analysis of the leading covariance eigenvectors of worldwide sea  
surface temperature anomalies for 1901-80.  
by C K Folland and A Colman (April 1988)